ijlpr 2023; doi 10.22376/ijlpr.2023.13.5.L176-L198

International Journal of Life science and Pharma Research

ISSN 2250-0480

Review Article

Growth Factor Scaffolds for Bone Tissue

A Review on Growth Factor Loaded Scaffolds for Rapid Healing of Bone Tissue

Yochana Boddepalli[1], Nikhitha Chava[1], Sarvani Gadiraju[1], Kavya Sri Pachchava[1], Karthik Kotikalapudi[1], and Nadeem Siddiqui[1]*

[1]*Department of Biotechnology, Koneru Lakshmaiah Education Foundation, Vaddeswaram, Guntur, Andhra Pradesh, 522502, India.*

Abstract: Artificial bone implants from various sources, including metals, polymers, and bio-ceramics, turned out to be extensively occupied in present-day tissue engineering applications. The biomaterials provide an essential platform for the osteoblast cells to multiply, increase, and differentiate into mature osteocytes leading to bone regeneration in the defect site. Apart from biomaterials and cells, the other essential component in tissue engineering is growth factors. Growth factors are the biomolecules responsible for transformation, growth, migration, and cell crawling on the biomaterial's surface. Many growth factors like BMP (Bone Morphogenetic Protein) family, (Transforming Growth Factor Beta) TGF-β, and VEGF (Vascular Endothelial Growth Factor) exhibit a crucial role in angiogenesis, extracellular matrix (ECM) formation and transformation of fibroblasts and other stem cells into osteocytes aiding in bone growth. In addition, the growth factors have higher renal clearance making it tough to maintain their levels at the site of injury, which demands a sustained release approach. Our review aims to explore various growth factors used in treating bone defects; the primary objective is to understand each growth factor's role in the healing process and tailor the scaffold according to the requirement. Further, in this review, we have focused on the growth factors being used, their importance, and the sustained release strategies being followed for the efficient distribution of growth factors and, thus, bone healing by covering the use of different growth factors in conjunction with biomaterials involved in the treatment of bone tissue defects.

Key Words: Growth factors, Biomaterials, Bone regeneration, Angiogenesis, Fibroblasts

***Corresponding Author**

Nadeem Siddiqui , Department of Biotechnology, Koneru Lakshmaiah Education Foundation, Vaddeswaram, Guntur, Andhra Pradesh, 522502, India.

Received On 28 January, 2023
Revised On 18 April, 2023
Accepted On 9 May, 2023
Published On 1 September, 2023

Funding This research did not receive any specific grant from any funding agencies in the public, commercial or not for profit sectors.

Citation Yochana Boddepalli, Nikhitha Chava, Sarvani Gadiraju, Kavya Sri Pachchava, Karthik Kotikalapudi, and Nadeem Siddiqui , A Review On Growth Factor Loaded Scaffolds for Rapid Healing of Bone Tissue.(2023).Int. J. Life Sci. Pharma Res.13(5), L176-L198 http://dx.doi.org/10.22376/ijlpr.2023.13.5.L176-L198

1. INTRODUCTION

Bone is an important connective tissue in the body consisting of calcium, phosphate, and other essential mineral components providing a basic structure and imparting stability to the body. Bone is of two kinds, namely spongy and compact. Bone tissue comprises a mineral phase supported by a collagen framework enabling the bone to be flexible and bendy without getting shattered. Bone is the utmost dynamic organ system in the body, consistently reserved by osteoclasts and subsequent regeneration by osteoblasts. This normal bone resorption and formation is a well-maintained cycle with essential support from Bone Morphogenetic Proteins (BMPs), various growth factors, and other nutritional requirements. The above cycle is also responsible for the healing of bone tissue due to fractures, and other deformities, which, if not balanced in regulation, leads to bone defects such as osteoporosis [1]. Osteoporosis is a global disorder originating from the extreme action of osteoclasts against osteoblast cells leading to more resorption and decreased bone density, thereby reducing the Strength of bone. The root cause of osteoporosis is the aging process of the animal system. Apart from osteoporosis, the other factors include bone tumors, traumatic accidents, and other bone-related disorders such as periodontal disease. Considering the above mentioned factors, bone injuries seem extremely common, increasing the risk of fractures and bone fragility [2]. Regardless of the colossal regeneration capacity of the bone cells, therapeutic intervention is required in case of large bone tissue defects where regeneration is not at its full potential. The autograft procedure was the go-to method for the treatment of such large defects until the recent past. Grafting the bone from another body part is a painful and risky process as a second surgery is involved, and the risk of infection is of the highest probability [3]. Due to the availability of healthy donor tissue and associated complications, synthetic bone replacements and support structures have gained enormous importance in orthopedics. They are ideal for treating fractures, bone tumors, and other bone-related disorders. The doctors dictating ideal characteristics include biocompatibility, mechanical Strength, osteoinductivity, and other material characteristics, which make it easy for the material to be molded into the required size and shape [4,5]. Biomaterial is a biocompatible material that induces bone growth and facilitates osteoblast proliferation, leading to an enhanced recovery rate. Most common biomaterials used include synthetic polymers like Polyvinyl alcohol (PVA), Polyglycolic acid (PGA), Polycaprolactone (PCL), Polylactic acid (PLA), and natural polymers like Gelatin, Alginate, Collagen, etc. Bio-ceramic materials like Wollastonite, bioactive glass, Hydroxyapatite (HAp), and β-Tricalcium phosphate (β-TCP) have also been widely utilized in tissue engineering applications [2,4,6]. Porous biomaterials can be utilized to design 3D scaffolds, which are ideal for supporting osteoblasts for adhesion, proliferation, and crawling. The scaffold should be designed by appropriate cells, Mesenchymal stem cells (MSCs), or osteoblast cells. Co-culturing of cells on the scaffold after the scaffold construction was identified as beneficial for tissue engineering strategy [3]. Growth factors (GF's) and cytokines play an important role. Synergetic interaction between GFs and the signaling pathways of the host system is the determinative factor for progressive bone repair. Most GFs are important in skeletal development during the fetal phase and play a key role in repairing injured bone tissue [7]. Amid the growth factors, Bone morphogenetic proteins (BMPs) are the crucial factors involved in inducing the transition of MSCs into matured osteoblasts. The Food and Drug Administration (FDA) of the United States has approved using these BMPs in tissue engineering-based strategies. BMPs 2 and 7 are the most widely used growth factors in the Transforming growth factor (TGF-β) family involved in osteoblast transformation, proliferation, hematopoiesis, neurogenesis, and skeletal morphogenesis. Apart from the functions mentioned above, they also regulate the differentiation of adipocytes, fibroblasts, neuroblasts, and myoblasts [8,9]. Apart from BMPs, other important growth factors convoluted in bone regeneration include Platelet-derived growth factor (PDGF) and Vascular endothelial growth factor (VEGF). VEGF has been directly linked to angiogenesis and the inflammatory immune response, much-needed factors in bone regeneration. It also directly impacts chondrocytes, osteoblasts, and osteoclasts, which all carry the VEGF receptors, thereby directly modulating the bone healing process. A direct outcome of VEGF on MSC proliferation and differentiation was reported during in vitro studies [10]. PDGF is an active cytokine that plays an important role in osteoblast recruitment to the site of injury and also acts as an initiator of mitosis in osteoblast cells. It also stimulates extensive vascularization at the injury site through angiogenesis by stimulating the VEGF molecules [7,11]. Despite possessing the qualities needed for supporting the bone tissue healing process, the short life of these growth factors in the blood and their renal clearance threshold limit their use to the fullest extent. The sustained acquittance of these growth factors is necessary to reach the desired outcome. The scaffold structure used should be biocompatible and also should provide sustained release. Nath et al. 2015 utilized the polyelectrolyte complex (PEC), comprising a complex of charged polymers with the strongest acids and bases, which are body friendly. Attaining fully ionized forms, the PECs act as excellent release materials for growth factors [11]. Polymer-bioceramic composites were also reported to successfully provide sustained release of GF's owing to their spongy nature. Other ceramics such as bioglass, borosilicate, and Hydroxyapatite were also successfully utilized with various polymers to provide constant growth factor release [16-20].

2. SCAFFOLD REQUIREMENTS FOR BTE

Scaffold is a support structure involved in providing an environment and architecture for the tissue to regrow and develop, as assessed by De Witte et al. An ideal scaffold is designed to provide good cell adhesion, better surface area, sustained release of growth factors, and good biodegradability. An ideal BTE system has the following important components, (i) a mechanically and chemically stable scaffold, (ii) growth factors to enhance cell growth, and (iii) the capability to promote vascularization for nutrient supply. Structural requirements of scaffolds include porosity which leads to interconnected network-like structures enhancing the surface area, nutrient transfer, and gas transfer; nanoscale topography enhances the surface area of the scaffold. Mechanical requirements of the scaffold include compressive Strength of approximately 2-12 MPa and Young's modulus of approximately 0.1-5 GPa. Physical requirements of scaffolds include biodegradability, where scaffold remains are gradually eliminated through body secretions, the ability to induce osteogenesis, and providing a nontoxic environment to bone cells [12]. The biomaterials for bone tissue repair include metals, polymers, ceramics, and composite materials.

2.1. Metals

Metals are extensively used in orthopedic applications, mainly in joint replacements, artificial spines, dental implants, and other load-bearing applications. They possess excellent mechanical, electrical, and thermal properties. Yet the main drawbacks of metallic biomaterials are their bio inertness, and they are very expensive [13]. The most extensively used metallic biomaterials are alloys of titanium, stainless steel, cobalt, nickel, and magnesium. Titanium and its alloys are the most widely used metallic biomaterials due to their great corrosion resistance in dental implants. Stainless steel(316L), cobalt, and nickel-based alloys are widely applied in various orthopedic and stent-based applications. Niobium-Zirconium alloys and tungsten-based alloys were also being used in the fabrication of medical equipment, given their superior corrosion resistance. Nickel and cobalt alloy-based stainless steel is also used to manufacture hip joints and other load-bearing implants. The other applications where metallic biomaterials are used include dental implants, bone fixation devices, craniofacial plates, prosthetics, and stents [14]. With great advantages, metallic biomaterials also have their fair share of drawbacks; upon contact with blood and host tissue, metallic implants erode, leading to implant failure. There are also problems associated with the leaching of metal ions into the bloodstream, which might lead to infections, inflammation, and many other allergic reactions, which can also be fatal if left unattended [15].

2.2. *Polymers*

Polymers are the second class of biomaterials widely employed in tissue engineering and regenerative medicine as scaffold structures and therapeutic drug delivery systems. They possess the advantage of being flexible, which enables them to take the desired size and shape, such as nanofibers, 3D scaffolds, hydrogels, etc. [16] Polymers also possess a few limitations, which include low mechanical strength and stability. In addition to stability, other drawbacks associated with polymers are sterilization and handling sensitivity [17]. Classification of polymers into Natural and Synthetic based on their source of extraction.

2.3. *Natural Polymers*

Natural Polymers such as Chitosan, Collagen, Alginate, Hyaluronic Acid, Cellulose, etc., are derived from natural resources and are being utilized in the field of BTE due to their better biocompatibility, low level of antigenicity, and proven capability of cell growth and differentiation [18]. Other parameters favoring natural polymers are their ability to impart porosity, desired charge, and ease of tuning of polymer concentrations to fabricate the scaffold of desired shape. They also exhibit adhesive properties with a large number of ligands. Various scaffold fabrication methods can be employed to develop natural polymer-based scaffolds, including fiber bonding, melt molding, solvent casting, gas foaming, phase separation, and electrospinning [19,20]. Natural polymers are the go-to biomaterials for hydrogel development. Hydrogels are 3D networks predominantly consisting of water and aid in homogenous cell encapsulation. They are also proven to mitigate surrounding tissue damage due to their soft texture [21,22]. Although possessing ideal biomaterial properties, natural polymers possess few limitations, including very low mechanical Strength and quick biodegradation [23].

2.4. *Synthetic Polymers*

Synthetic polymers such as PLA (PolyLactic Acid), PGA (PolyGlycolic Acid), PCL (PolyCaprolactone), PMMA (Polymethyl Methacrylate), etc. are derived from artificial sources. Synthetic polymers exhibit better properties of tensile Strength, lower biodegradability, and higher mechanical stability than their counterparts which possess poor mechanical strength and stability. Based on degradability, polymers are classified into biodegradable and nonbiodegradable polymers. Biodegradable polymers degrade in host tissue over time, and the degradation products are not toxic to the host tissue. Non-biodegradable polymers take a very long time to degrade and also possess an additional limitation of the degradation byproducts being toxic to the body. They also pose a limitation of being hydrophobic, with an example being PLA possessing a high degree of hydrophobicity, leading to poor cell adhesion to the surface [18,24,25,26].

2.5. *Structure of Polymers*

As mentioned above, natural and synthetic polymers have been extensively used in BTE due to their outstanding features of biocompatibility and flexibility. Structures of a few natural and synthetic polymers are illustrated in Figure 1.

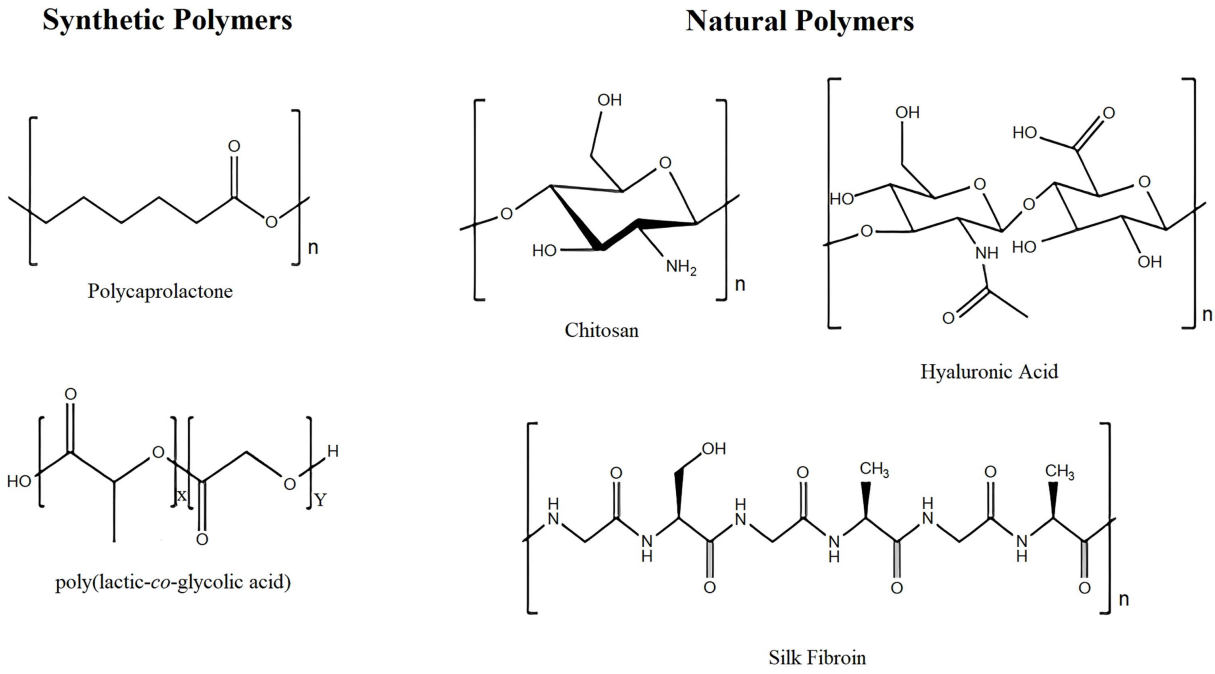

Fig 1: Structures of a few commonly used Natural and Synthetic Polymers [21].

2.6. *Bio-Ceramics*

Ceramic biomaterials can be classified as Inert ceramics, Porous ceramics, bioactive ceramics, and Resorbable ceramics. Aluminum and Zirconium fall into the category of bioinert ceramics as they do not support cell adhesion and lead to the formation of fibrous layers at the implant host tissue interface. Bioactive ceramics such as Bioactive glass, Hydroxyapatite, and β-TCP are porous and known to bond directly to the host's residual bone tissue, leading to enhanced cell proliferation at the interface and deep into the porous structure of the ceramic. Plaster of Paris was used as setting material to treat fractures previously. Still, in modern days, various bioceramics are being used to treat bone defects, including Calcium Phosphates, Diopside, Wollastonite, Bioactive glasses, etc. [27] The Bioactive glass synthesized by Larry Hench bonds with the host bone tissue via direct chemical bonding. This strong bonding is a consequence of the dissolution of bioactive glass in the physiological environment, and the dissolution products lead to the formation of the HCA (Hydroxycarbonate Apatite) layer promoting osteogenesis [28]. Bioceramics are corrosion resistant, unlike their metallic counterparts, but have a few limitations: brittle, high stiffness, and susceptibility to fractures. Addressing the drawbacks mentioned above is a major challenge. Among all the bioceramics mentioned above, bioactive glass is the most commonly used ceramic as it has higher load-bearing strength than its ceramic counterparts of HAp and β-TCP, the other commonly used ceramics [29,30]. Classification of Biomaterials is illustrated in Figure 2, and a summary of various biomaterials with their pros and cons is depicted in Table 1.

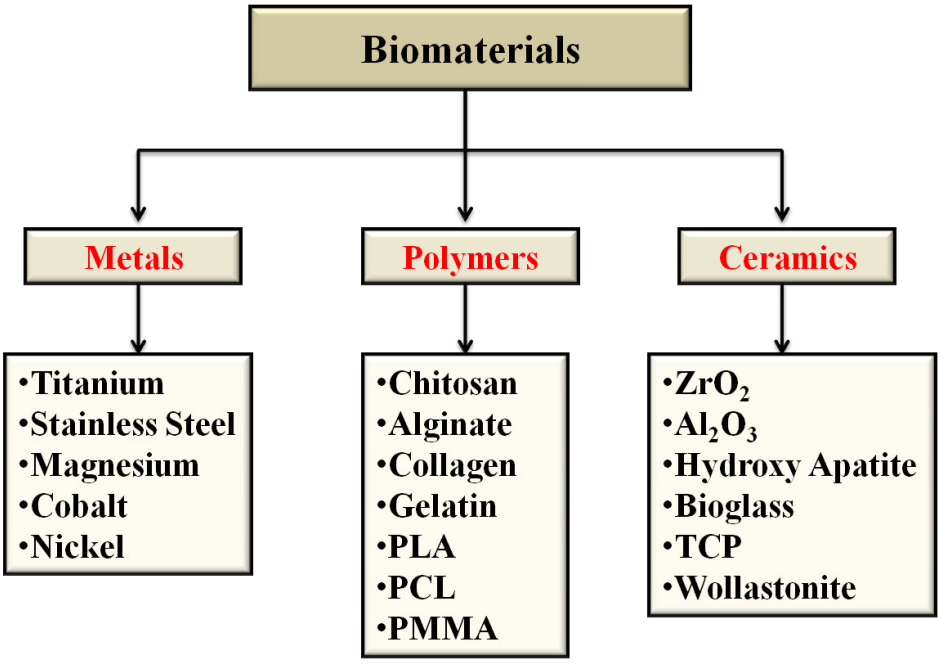

Fig 2: Classification of Biomaterials with suitable examples.

Table 1: Summary of Biomaterials Employed in Bone Tissue Engineering with Advantages and Limitations

Scaffold Material	Examples	Advantages	Limitations	References
Metals	Titanium Stainless Steel Cobalt Nickel Magnesium	Mechanical Strength, Greater Electrical and Thermal conductivity,	Bio-Inert in nature, Expensive to fabricate	13 14
Natural Polymers	Chitosan Alginate Collagen Gelatin	Flexible to mold Biocompatible and Biodegradable	Low Mechanical Strength Faster biodegradation	16
Synthetic Polymers	PLA PCL PMMA	Flexible to mold Biocompatible and longer lifetime	Very slow biodegradation Not so effective in cell interactions as natural polymers	24
Bio-Ceramics	Bioglass β-TCP, HAp, Al_2O_3, ZrO_2	Strong chemical bond with the bone Bioactive and Bioresorbable	Brittle in nature, leading to low fracture toughness High stiffness	27

Table 1 summarizes the various biomaterials used, i.e., Metals, Polymers - Natural and Synthetic, and Bioceramics. Notable advantages and disadvantages of each type of biomaterial are presented, along with relevant examples and references.

3. INCORPORATION AND DELIVERY OF GROWTH FACTORS

BTR initiation depends on the GF's, which contribute to the signaling process by leading inflammatory and progenitor cells to the implantation [18]. These GFs dictate cellular behavior by promoting effective binding with transmembrane receptors of target cells. The regulation is in the form of short-range diffusion via the ECM [31]. It can be deduced that apart from fabricating the scaffold to mimic the ECM, it is also important to incorporate the growth factors, including inflammatory, angiogenic, and differentiation agents [32]. The main limitation associated with direct localized delivery by injections is the short life of the GF's in vivo and the adverse effects associated with the formation of heterotrophic bone. Local inflammation and osteoarthritis [33,34]. Developing efficient delivery systems to mitigate the adverse effects and provide sustained release leads to decreased overuse of GFs, thereby decreasing the chances of excessive bone growth and side effects caused due to excessive GF delivery [35]. Further discussion on Angiogenic and Inflammatory factors is given in the upcoming sections. The role of growth factors in bone regeneration is represented in Figure 3.

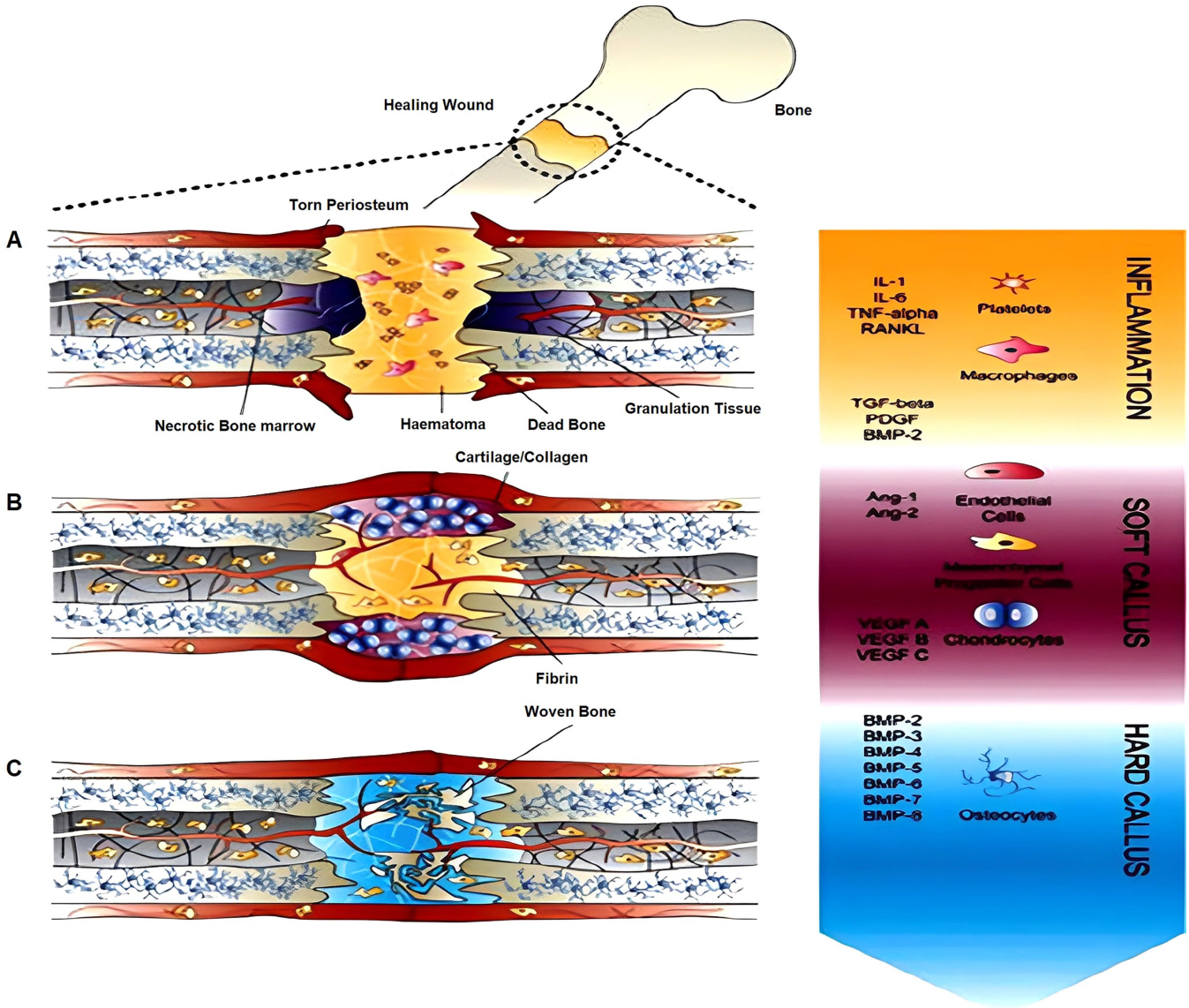

Fig 3: Representation of stepwise Bone Regeneration. (A) Inflammatory Stage, (B) Soft callus formation stage, and (C) Hard callus formation stage.

The figure was reproduced from the work of Lienemann et al. 2012 [36].

4. ANGIOGENIC FACTORS

Bone is an avascular tissue, i.e., it lacks blood vessels leading to its reduced regeneration ability, a condition also referred to as ischemia. The function of vascularization is limited to the supply of nutrients and oxygen and the enhancement of signaling for the proliferation and differentiation of osteoblasts [37]. Angiogenesis is a key mechanism for forming new blood vessels from preexisting ones. This process is essential for providing nutrients, oxygen, and growth signals to the developing osteoblasts [35]. The key angiogenic factors involved in BTR are PDGD, FGF, BMPs, and VEGF [36]. The mechanism of action of these growth factors was given in the introduction section.

5. INFLAMMATORY FACTORS

Inflammation is the first step of repair to any tissue defect in the body, including bone tissue repair. It can be observed for the first few days post-bone fracture [37,38]. Damage of blood vessels during the injury leads to internal bleeding followed by clotting of blood at the injury site. Blood clotting is associated with platelets, which produce proinflammatory cytokines that attract the lymphocytes, macrophages, osteoclasts, and plasma cells [39]. The major proinflammatory cytokines involved in inflammation include the TNF-α, which is responsible for osteoclast activity, FGF-2, IL-1, IL-6, and Macrophage-CSF [36].

5.1. Role of Growth Factors in Conjunction with Natural Polymers for rapid bone healing

Honda et al. studied the effect of Leukocyte platelet-rich fibrin on cell responses (Htrtert-MSCs) and its capability to repair bone defects reviewed in rats. Expression of certain genes such as ALP, OPN, and COL1A1 was significantly increased by treatment of 5-20%, 5-10%, and 3-5% concentrated CGF extract, respectively (qPCR). A significant increase in hTERT-E6/E7 cell proliferation and calcification is observed at 1-10% and 3-10% concentrations of CGF extract, respectively, indicating the repressive effects of CGF extracts at higher

concentrations. Authors have also investigated the bone regeneration capacity of CGF and CGF with BMSCs in rat calvaria critical-size defects. The formation of new bone and calcified volume of neo-bone formation was determined by microfocus CT and Tri/3D Bon software, respectively. The neo-bone formation was observed only at the periphery of the defect in control. In the CGF group, new bone accumulation started at the periphery and moved toward the center of the defect. The bone healed completely in 12 weeks, indicating the role of CGF in bone regeneration [40]. An injectable chitosan nanoparticle (200-300 nm) encapsulated Gellan-Xanthan gels were prepared and loaded with BMP-7 and bFGF to assess the effect of varied concentrations (0.5, 0.7, and 0.9%) of gel on cellular responses of L929 osteoblasts. A significant decrease in the release of BMP-7 on chitosan nanoparticles having scaffolds (27) compared to scaffolds without chitosan (80), indicating constant discharge of GF on prepared scaffolds. The authors have reported an increase in elastic modulus with a rise in gel concentration. Further, results of In vitro cell viability (MTT & Live and Dead assay) have exhibited an increased viability of both types of seeded cells on scaffolds with both the growth factors compared to scaffolds with one growth factor and no growth factor. In addition, increased ALP activity and mineral deposition on scaffolds with BMP-7 containing scaffolds as a contrast to scaffolds with bFGF and the corresponding ALP values are 23 and 17 nm/ml, respectively [41]. Roche and his co-researchers developed a Keratose/BMP-2 composite scaffold, an alternative biomaterial for Infuse bone graft (Collagen I/BMP-2) with superior qualities compared to infuse. Authors have compared the release profile of BMP-2 on these developed scaffolds and suggested an increase in the GF release on Keratose-based scaffolds compared to contrast during the initial time points, followed by no indicative difference in both the groups of scaffolds. Further, the authors also reported an increase in bone volume 25-fold when BMP-2 concentration was doubled (25-50 µg) during implantation of the composite scaffold in the hamstring muscle of mice. Furthermore, implantation in the femur of mice has suggested an increased level of mineralization density (~1.5 times), Bone mineral content (~1.45 times) on Keratose based scaffold as compared to Infuse bone graft and uninjured tissue (control), indicating the role of keratose based scaffolds in BTR [42]. The research aimed to investigate pure chitosan's effectiveness and bone regeneration capacity along with insulin-like bone morphogenic protein (BMP-2) and growth factor (IGF-1). The Chitosan scaffold was fabricated by a simple liquid hardening method, and growth factors were incorporated into the scaffold using vacuum infiltration with the freeze-drying method. SEM results demonstrated a decrease in pore size and hardening of chitosan scaffold when impregnated with GF's. Average pore sizes of pure chitosan (group-A), chitosan/IGF-1 (Group-B), and chitosan/BMP-2 (Group-C) were obtained to be ~350, 75, and 125 µm, respectively. The type of attachment of GF on the plane of the chitosan scaffold was examined using FT-IR, and they found that IGF-1 and BMP-2 are attached to the chitosan scaffold by hydrogen bonding and physical adsorption, respectively. Adsorption efficiency values depicted more adsorption of IGF-1 to the chitosan matrix compared to BMP-2. Further, authors have also investigated in vivo efficacy of developed scaffolds using rabbit models to evaluate and compare the efficiency of 3 groups of scaffolds. Radiographic observation showed a significant decrease in gap size by new bony tissue, proof of radiodensity in the damaged area from the 60th day in groups B and C compared to group A. Histological observations showed the proliferation of osteoblast and fibroblast in bony sections of groups B and C. Sufficient vascularity around the haversian canal is observed in group B, followed by groups C and A, respectively [43]. Qin Shi et al. prepared BMP-2 loaded cellulose (BACTERIA) based scaffolds to assess the osteogenic differentiation ability of mouse fibroblast-like C2C12 cells. Cell proliferation in scaffolds with GF is higher when compared to scaffolds without any GF and control (only media). Results of ALP have suggested an A linear relation with BMP-2 concentration. Further, in vivo, implantation (subcutaneous) of 3 different groups in the rat model inferred the result of BMP2 concentration in bone tissue regeneration. The percentage of calcification on a low dose (225 µg/ml) and high dose (450 µg/ml) GF-containing scaffold was 18.9% and 26.5%, respectively [44]. Fenglin et al. developed chitosan-based hydrogel with basic transforming growth factor β3 (TGFβ3) and fibroblast growth factor (bFGF) entrapment-filled chitosan microspheres to treat periodontal tissue defects. A group of bFGF and TGF β3 indicatively raised the mineralization promotion and osteogenic differentiation ability of hPDLSCs (human periodontal ligament stem cells). bFGF was almost completely released in 7 days, whereas only 55% of TGF β3 was released in 14 days. The amount of new bone tissue, bone volume fraction (18%), trabecular number (0.03nm^{-1}), and trabecular thickness (6µm) of new bone was significantly higher in GF-loaded hydrogel groups in comparison to scaffolds without GF's (5%, 0.01nm^{-1}, 4 µm) as reported by authors [45]. Li and his team have incorporated Icariin (osteogenic flavonoid) into collagen (extracted from small intestine submucosa-SIS) and studied the impact of Icariin on new bone growth in mouse calvarial imperfection models. In addition, results of viability and differentiation (ALP, BSP, OC, and OP expression by RT-qPCR) of seeded MC3T3-E1 cells have shown a higher cell proliferation and differentiation on a thick layer of a scaffold containing Icariin as compared to the scaffold with thin layered SIS. Furthermore, in-vivo results have shown an enhanced bone regeneration in C57BL/6 mice (calvarial defect model) in scaffolds with Icariin compared to pure SIS and control group for a period of 8-week implantation. (46). Kim et al. have advanced a collagen scaffold in which VEGF165 was incorporated with the help of a silica nanoparticle (CMV scaffold) which has 654.5µm of pore size and 84.4% porosity. In 26 days, the scaffold released 56% of the total weight of 250mg. rat mesenchymal stem cells (MSC) were cultured, and the authors reported an increase in bioactivity observed on the scaffold with VEGF compared to the VEGF-free scaffold. [47]. Masako and team have developed Hyaluronic acid loaded BMP9 and compared its carrying capacity with TCP. Through SEM images, they interpreted that the rhBMP9 growth factor is well attached to Hyaluronic acid scaffolds and has shown a controlled release. Further, authors have reported a two-fold increase in cell proliferation on HA/rhBMP9 compared to TCP and pure HA. ALP activity assay showed that ST2 cell differentiation (pre-osteoblasts studies) rate is high in HA/rhBMP9 scaffold along with 4 folds with higher expression of collagen 1α2 (COL1a2), ALP, and OCN markers. In contrast, HA scaffolds have shown less differentiation and gene expression. [48]. Farnaz and team developed glutaraldehyde (GA) conjugated silica containing human platelet particles (PRP) scaffolds (CL-PRP/SiO_2) and cultured MG63 cells. Authors inferred the part of surface roughness in cell proliferation and adhesion, and the SEM images depicted the same. Alizarin red staining and Alkaline phosphatase assay also showed that Non-CL PRP/SiO2 scaffold showed a high amount of calcium deposition and osteoblast formation, respectively, when compared to the CL PRP scaffold, Non-CL PRP scaffold, and CL PRP/SiO2 scaffold,

suggesting that silica presence leads to better bone formation [49]. Kim and his co-workers fabricated bovine bone powder and fibrin glue (FB) scaffolds. They loaded the scaffold with Angiogenin (ANG) to assess its part in promoting bone regeneration and angiogenesis. H&E, Masson trichrome staining and micro-CT observations have depicted an increased blood vessel formation along with bone mineralization on FB/ANG (2.0µg) scaffold compared to other scaffolds when implanted in rabbit calvarial defect as reported by the authors [50]. Qing Li developed a freeze-dried deproteinized bovine bone scaffold (DBB) incorporated with chitosan microspheres (CM), followed by loading with BMP-2. Good cell adhesion was noted on DBB/CM/BMP-2 when seeded with MC3T3-E1 cells. In addition, qPCR analysis reported an increased release of osteogenic markers (ALP, BMP-2, OCN) on DBB/CM/BMP-2, which indicates MC3T3-E1 has been differentiated and thus the potentiality of scaffold for Bone Tissue Engineering applications [51]. Mari Carmen and his team prepared transglutaminase (mTG) cross-linked gelatin-based scaffolds using different proportions of Gelatin (10 to 20% w/v) and cross-linker concentrations (10 and 30U/g). BM-MSC (bone marrow mesenchymal stem cells) were loaded onto the scaffolds. The outcomes of CCK-8 assay and RT-PCR have shown higher cell viability and osteogenic differentiation ability (expression of Col1a1, Runx2, and Osx mRNA and reduced the expression of Oct4 and Nanog markers) on GEL_10/20 (10% w/v Gelatin & 20u/g crosslinker concentration) scaffolds as compared to GEL_20/20 (20% w/v Gelatin & 20u/g crosslinker concentration). Growth factor Entrapment efficiency on GEL_10/20 scaffolds (92%) is higher when compared to its counterpart (61%) [52]. Aziziana and her team prepared basic fibroblast growth factor (bFGF) and bovine serum albumin (BSA) integrated with chitosan nanoparticles into a chitosan-gelatin scaffold. Researchers also observed a gradual decrease in water contact angle upon adding chitosan particles, indicating increased hydrophilicity. They also observed the release pattern of BSA and stated that the release was around 80% within a week, which declined after 2 weeks. Results of MTT assay and SEM images have shown an increased proliferation rate and better cell adherence on FGF-containing scaffolds compared to scaffolds without any growth factor [53]. Menemse and his team designed the heparin-functionalized chitosan scaffolds and examined the activity of MC3T3-E1 on the scaffolds. The SEM images showed that the chitosan scaffolds possessed a pore size and a porosity of about ~100µm and 82%. In 3 days, 45% of the heparin was released, and 71% was released during 20 days. The authors also reported that the compression modulus before and after modification was 1.993 ± 0.035 N/mm^2 and 2.853 ± 0.429 $N/mm^{2,}$ respectively. Further, preosteoblasts were seeded onto the scaffolds, and their viability was determined by performing an MTT assay. Further, a similar trend of ALP activity and expression of OCN (osteocalcin) is also noticed, indicating the significance of interactions with the scaffold and, thus, the potentiality of developed scaffolds for tissue engineering applications [54]. Zhang and his team constructed recombinant BMP2-loaded cellulose nanofibers and studied the effect of aligned and random fibers on cellular responses in-vitro and in-vivo. Besides, the BMP2 release profile on random and aligned nanofibers was 0.76µg and 0.74µg, respectively, in a time of 7 days suggesting no significant difference. Further, BMSCs were seeded onto the scaffolds, and the mineralization capacity of BMSCs was investigated by performing ALP activity and observed that aligned and random fibers with BMP2 have shown increased values (10.89 & 9.678) when compared to scaffolds without any GF (4.168 & 4.915). Moreover, in vivo study was examined for bone regeneration, thereby implanting the scaffolds in the defect region (calvarial defects of rabbit), and reported that Bone volume (BV) and bone mineral density (BMD) were high for aligned and unaligned scaffolds loaded with BMP2 (8.63 mm3, 14.09 g/cm3, and 7.62 mm3, 12.15 g/cm3) compared to non-loading groups (5.58 mm3, 8.12 g/cm3, and 5.22 mm3, 7.64 g/cm3) [55]. Park and his team prepared 3D plotted Alginate hydrogel containing BMP2 and MC3T3 osteoblast cells with 500-980 µm. 90% of BMP2 is released from the hydrogel by the end of 2 days. Results of in vitro studies have proved that the proliferation of cells seeded on growth factor-containing scaffolds was higher than in pure hydrogels. A 2-fold rise in ALP activity of MC3T3 cells was observed on scaffolds with growth factors compared to virgin scaffolds [56]. Sharmila and her team prepared a plant extract (*Spinacia oleracea* and *Cissus quadrangularis*) loaded with Alginate/CMC composite porous scaffold by Freeze drying. Plant extracts were an exact mimic of growth factors that assist in the proliferation and differentiation of MG-63 Human osteosarcoma cells, as reported by the authors based on the results of MTT (94.55% and 77.62%) [57]. Laura and her team fabricated the silk fibroin (SF) scaffolds incorporated with a Gasotransmitter, signaling molecule GYY4137 at two different concentrations and assessed the cellular responses with a rise in the concentration of GYY4137, with a pore size range of 80-350µm. H_2S release from the scaffold with 1.25 and 5% Gasotransmitter was 3.5 and 10µM, respectively. Moreover, hMSCs (human mesenchymal stromal cells) were grown on these scaffolds. The results have suggested increased cell viability and production on scaffolds with advanced concentrations of GYY4137 compared to pure and low concentrations of GYY4137. Furthermore, a 2-fold increase in the appearance of osteogenic (ALP, BGLAP, RUNX2, DLX-5, BMP-4, BMPR1A, BMPR2, and COLLXV) and angiogenic (FLT-1) markers have been reported by the authors on scaffolds with a higher level of Gasotransmitter as compared to its counterpart [58]. By freeze-drying, Ciara developed bmp2 and ZA (zoledronic acid) enriched collagen hydroxyapatite (CHA). Despite adding Zoledronic acid, there was no significant change in cell viability when they used MC3T3E1 cells. Varied concentrations of ZA(5-10ug) and BMP-2(5-10ug) were used to prepare composite scaffolds implanted subcutaneously in the rat's hind limb. Higher amounts of bone formation were noticed on the 10 ug ZA/10ugBMP-2/CHA scaffold compared to other concentrations. further, there is a significant reduction in osteoclast number, suggesting the change in bone metabolism leading to fast bone growth on 10 ug ZA/10ugBMP-2/CHA scaffold [59].

5.2. Role of Growth Factors in Conjunction with Synthetic Polymers for rapid bone healing

Eshan et al. developed VEGF incorporating materialized PLAGA (poly(lactide-co-glycolide) scaffolds capable of mimicking natural ECM and delivering an angiogenic factor. PLAGA sintered microsphere scaffolds were mineralized by incubation in modified SBF. Mineralized PLAGA scaffolds are shown on rougher surfaces with well-defined nanostructured plate-like structures compared to non-mineralized PLAGA scaffolds, as confirmed by microscopic images. As reported by the authors, PLAGA and mineralized PLAGA scaffolds possess similar compressive modulus & strength (402 $\pm$ 61 MPa; 14.6 $\pm$ 2.9 MPa). Initial VEGF burst discharge (7^{th} day) was observed in mineralized and non-mineralized PLAGA scaffolds. However, a reduction in the initial burst release of VEGF was

set up for mineralized PLAGA scaffolds (89.1 % to 71.2%). VEGF-loaded mineralized PLAGA scaffold showed greater cell proliferation (endothelial) and higher metabolic activity than its counterparts. Furthermore, RT-PCR analysis revealed that endothelial gene expressions of PECAM-1, Vwf (von Willebrand factor), and inflammatory cell adhesive molecules such as ICAM-1 and E-selectin were significantly higher on mineralized scaffolds than PLAGA scaffolds [60]. Sinan et al. prepared Poly-L-Lactide- Polyethylene glycol (PLA-PEG-PLA) copolymer scaffold by freeze drying and filling with both vascular endothelial growth factor (VEGF) and bone morphogenetic protein (BMP-2) and cultured MC3T3-E1 mouse osteoblast cell. They used salt leaching techniques to prepare different concentrations of copolymer (3.0%,5.0%,8.0) and noted that scaffolds with 5% copolymer solution were optimal for good porosity, interconnectivity, and good mechanical stability. Sinan and Numan achieved their goal through fast delivery of VEGF up to 60% within 2 days and prolonged slow release of BMP-2 up to 100 days. They compared VEGF/BMP-2 containing scaffold with pure scaffold and observed that cell proliferation occurs in both. Still, due to rough and pores formation by VEGF and BMP-2 cell proliferation, interconnectivity between pores and osteoblast attachment is high. When tested with the double staining method, more intensity of blue color in loaded scaffold VEGF/BMP-2 was observed, indicating more healthy cells and the absence of red color, indicating the absence of necrotic cells compared to its counterpart [61]. Shudham et al. prepared a poly ε-caprolactone (PCL) nanofiber scaffold incorporated with curcumin (phenolic compound-improve bone microarchitecture and mineral density) using electrospinning technology and cultured MC3T3-E1 cells. Shudham and team compared PCL solution (CU0), PCL with 1% curcumin (CU1), and PCL with 5% curcumin (CU5) and studied under SEM and observed that as the concentration of curcumin raised, the diameter of the fibers decreased from 835 nm to 680 nm respectively indicating that conductivity increases as the concentration increases. They observed that CU5 released 55µg/ml and CU1 released only 25µg/ml of curcumin, suggesting that CU5 is recommended for sustainable release. The SEM results indicated that cells had covered the entire scaffold area on CU0, but CU1 and CU5 showed cells are thinly dispersed on the scaffold, advising that high concentration is not useful for bone regeneration; moreover, it may cause damage to the cells. MC3T3-E1 cell differentiation was observed to be highest for CU1, followed by CU0 by alkaline phosphatase assay (ALP) analysis. Alizarin Red S (ARS) dyeing showed that the amount of mineralization is maximum at CU1 compared to CU0 and CU5. Energy-dispersive X-ray spectroscopy (EDS) reports confirmed the amount of Ca and P deposition is maximum in CU1, followed by CU0, which indicates that only certain concentrations are optimal for osteogenesis [62]. Michael and the team prepared a PLGA scaffold coated with PEM (multi-layered polyelectrolyte film) containing BMP-2. The prepared PLGA tube coated with PEM film containing 1-ethyl-3 carbodiimide (EDC) of 10, 30, and 70 concentrations is then loaded with BMP-2 into 4 different films, i.e., BMP5, BMP25, BMP50, and BMP100. Fluorescence spectroscopy showed that the growth factor content filled into the scaffold does not depend on EDC. Still, the concentration of BMP-2 discharge completely depends on cross-linkers, proved by noticing EDC10 releasing the highest growth factor and least from EDC70. They observed the new bone formation by taking different dosages of BMP-2 in a femoral bone defect in rats. They showed that cortical bone and its thickness formation depend on the growth factor concentration. Through ALP assay, they observed the bioactivity of cells, which is dependent on the concentration of BMP-2. Hence new bone formation is maximum in EDC10/BMP100 compared to other concentrations. µCT results showed that the concentration of EDC does not affect the formation of new bone tissue. However, BMP does. The amount of bone healing and outer cortical bone formation in BMP50 and BMP100 is high (1OO) compared to scaffolds with 25 percent BMP2 (62.5). Furthermore, authors have reported no significant effect of BMP2 on inner cortical bone formation as observed in their in-vivo studies [63]. Sang-jin and team plotted a polydopamine (DOPA) layered polycaprolactone scaffold (PCLS) loaded with rhBMP-2 and cultured MC3T3-E1 cells for 28 days. They observed the bone repair capacity of the scaffold by comparing it with the PCL scaffold; DOPA layered PCL scaffold, DOP-PCL-rhBMP-2 100 ng/ml (PCLSD100), and DOP-PCL-rhBMP2 500 ng/ml (PCLSD500). SEM images revealed that PCL has 500µm of pore size. Because of DOPA, the water contact angle of the PCL scaffold was almost zero, indicating good hydrophilic nature and good attachment of rhBMP2. They noted PCLSD500 scaffolds have a high impact on the growth factor uptake, and 79.7% of rhBMP-2 is released from the PCLSD500 scaffold within 28 days. Irrespective of the concentration of BP2 (1 ng/ml, 10 ng/ml, 50 ng/ml), no toxicity was observed for seeded cells, as reported by the authors. Further, the CCK-8 assay indicated that the percentage of cell proliferation is maximum in the PCLSD500 scaffold, followed by the PCLSD100 scaffold. ALP assay showed that rate of cell differentiation is high in PCLSD500 scaffolds indicating differentiation is dose-dependent. rt-PCR outcomes showed that the collagen type-1, BSP, osteocalcin (OCN) protein expression is always higher on PCLSD500 scaffolds indicating PCL scaffolds are recommended for bone tissue engineering [64]. Rampichová et al. prepared a 3-D poly-e-caprolactone scaffold loaded with varied platelet concentrations (10-100 times diluted 10^2 concentrated platelet-PCL/P1, PCL/P2, PCL/P3, PCL/P4, and PCL/P5) and cultured MG-63 cells for Bone Tissue Engineering. Authors have observed that cells' viability depends on the dosage of growth factor loaded onto the scaffold for better healing. Further, the scaffolds' average diameter, pore size, and porosity were 504 nm, 7.11µm^2, and 20%, respectively. ELISA results showed that 94,200pg/ml of thrombospondin growth factor is expressed, which is higher than other growth factors. As the release of thrombospondin is high in the scaffold, it is used to assess the rate of growth factor released and observed. MTS and ALP assay outcomes revealed that the rate of MG-63 cell proliferation and thrombospondin release (260000 pg/ml) is maximum in PCL/P1 scaffold compared to its contrast indicating its dependence on dosage for bone development [65]. Rahman prepared soybean lecithin(biosurfactant) incorporated with BMP-2 and loaded onto PLGA-PEG/PCL scaffold (bioactive osteo polyester scaffold-BPSC) using solid-liquid separation. Different concentrations of PLGA-PEG and PCL were taken ranging from 5%w/v-15%w/v to prepare 3 different scaffolds (BPSC, SC-BMP2(free BMP), SC (only scaffold)) for characterization, invitro, and in vivo studies. Scaffolds with 10w/v% concentration had shown a uniform pore size even when growth factors were incorporated. 10%BPSC have depicted a higher porosity (97%), higher swelling ratio (850%) and greater encapsulation efficiency (178 ng/ml), and slow degradation (90% IN 30 days) compared to others. CLSM images indicate that more mADMSC'S (mouse adipose-derived mesenchymal stem cells) were captured on BPSC.Future good cell viability and migration were noticed on

BOSCH OPSC express osteogenic markers, which indicate differentiation of mADMSC'S [66]. Xialin et al. studied BMP2 attached BMP-7 incorporated PELA scaffolds for treating defects in rat femurs and evaluated the impact of dual GFs. Further, the release of BMP-2 (81%) is greater than BMP-7 (74%) in 22 days, suggesting the role of attaching GF to a scaffold. Cell viability (MTT) and differentiation (AKP assay) of seeded MC3T3-E1 were higher on scaffolds with 2 GFs (2.7mg/ml) as compared to individual (1.7 and 2 mg/ml) and pure scaffolds as reported by Xialin and his team. In addition, micro-CT and Histological examination results revealed a higher bone mineral density (550mg/cc) and bone volume (60) on the scaffold with multiple growth factors (8 weeks) as compared to its counterpart (400mg/cc and 25) [67]. Kim and his team fabricated PCL/PLGA scaffold having pore size(150-200µm) and porosity (62.5%) with heparin dopamine mix (Hep–DOPA) for the delivery of BMP-2. They reported the controlled delivery of GF was because of the connections between negatively charged heparin and positively charged bmp-2. The Overall discharge of bmp-2 from Hep–DOPA/PCL/PLGA/BMP-2 (20.563 ng) was greater at the end of 28 days compared to Hep/PCL/PLGA/BMP-2 (16.55 ng), as reported by Kim and his team. Good cell viability (90%), enhanced ALP activity (0.94um/min/ug-day14), and the highest calcium deposit (10µg/nm) were noticed on Hep–DOPA/PCL/PLGA/BMP-indicating good responses of MG-63 cells. In addition, the highest bone volume and callus formation was noticed on Hep–DOPA/PCL/PLGA/BMP2 (85%, 0.45g/cm^3) compared to Hep/PCL/PLGA/BMP2(60%, 0.3g/cm^3), PCL/PLGA(40%, 0.19g/cm^3) when implanted in mice (critical-size cranial defect).Woven bone formation was reported on PCL/PLGA scaffold after 8 weeks of implantation [68]. Murphy and his team prepared scaffolds using poly (lactide-co-glycolide-PLG). They assessed mineralization as well as the effect of VEGF on responses of human dermal microvascular endothelial cells (HMVECs). As reported by the authors, VEGF from mineralized SBF scaffold was much less than that of mineralized PBS scaffold. HMVEC (human dermal microvascular endothelial cells) cells were seeded onto three different scaffolds, namely mineralized and non-mineralized VEGF-containing scaffolds (MV and NV) and mineralized scaffold without VEGF (MC- control). Mineralized and non-mineralized scaffolds with VEGF have shown better cell responses (Cell number, MTT, Proliferation, etc.) and a higher proliferation than their counterparts. In addition, MV and NV scaffolds released about 70% of VEGF in two weeks compared to the mineralized scaffold devoid of growth factor [69]. Basmanava and his team constructed poly (4-vinyl pyridine) and alginic acid microspheres consisting of BMP2 and BMP7 loaded into PLGA scaffolds. It was noted that microspheres with low concentrations (4 & 6%) had released more GF (100%) compared to higher concentrations (8 & 10%) which released only 59% and 41%. Also, microspheres prepared at different cross-linking duration (30min/60min) and temperatures (room temperature/4°c) displayed that ~30-70% content has been released along with a 2-fold increase upon temperature reduction to 4°c. Further, microspheres (4% and 10%) along with BMSC cells were embedded in foams and noted that irrespective of the absence or presence of the growth factor, the cell proliferation (Alamar blue assay) was observed to be highest in the foams containing microspheres. Apart from that, higher ALP activity was observed in both single (13 and ~11) and dual (~5.5) loaded growth factors compared to their counterparts (~9, 5, and 2) [70]. Kanczler and his team designed PLA (poly (DL-lactic acid)) scaffolds and incorporated vascular endothelial growth factor (VEGF) to investigate bone regeneration. Besides, authors have also evidenced a rise in cell viability, type I collagen appearance, and blood vessel formation by immunofluorescence, alcian blue/Sirius red staining, and vWF immunostaining in PLA scaffolds binding with VEGF along with seeded HBMSC cells when compared to the counter-parts. Further, human bone marrow stromal cells (hBMSC) were loaded onto the scaffolds and observed that pristine PLA and PLA with hBMSCs displayed less bone growth when compared to VEGF-embedded PLA scaffolds with hBMSc, which showed enhanced and remarkable new bone growth as well as bone-repair as suggested by the team. The authors also found new bone formation in VEGF/PLA-HBMSC scaffold in contrast to the other scaffolds by staining the scaffolds with Goldner's trichrome [71]. Zhang and his team developed BMP2 and Sphingosine (osteoinductive chemical compound) loaded poly-L-lactide (PLLA) scaffold with fiber diameter and compressive Strength of 108µm and 163.9-342.6kpa, respectively. GF release was approximately 20-25% in 3 days and 39% in 4 weeks, indicating a controlled release. BMSCs were seeded onto the scaffolds and observed that in contrast to the PLLA scaffold, cell viability (CCK-8 assay) and osteogenic differentiation ability (~1) more in the scaffolds with growth factors as a contrast to pure PLLA scaffolds. Also, the scaffolds were implanted subcutaneously into mice and reported neo-tissue formation by the end of 8 weeks. In addition, Histological analysis with H&E staining has shown the formation of trabecular bone at the implantation site in 16 weeks, advising the role of dual growth factors (sphingosine BMP2) in ectopic bone formation. Furthermore, authors have reported the expression of angiogenic markers like CD31 and Vwf, indicating neovascularization [72]. Sambit and his team prepared PLGA/bFGF coaxial nanofibers and compared them with blended fibers concerning materials and cell-supportive properties. SEM and AFM images have shown that both types of scaffolds possess a fiber diameter of 100-500 nm. Also, both the scaffold groups had an encapsulation efficiency of about 54%, as reported by the authors. Further, rabbit BMSc was seeded onto scaffolds, and the results displayed that the scaffold incorporated with bFGF showed enhanced cell proliferation (Live dead staining) compared to the counterpart. Further, collagen secretion by the seeded cells was higher on PLGA/bFGF coaxial nanofibers compared to PLGA/Bfgf blended nanofibers using circle assay, as reported by the authors. Furthermore, enhanced levels of collagen I and Fibronectin expression (qRT-PCR) on PLGA/bFGF coaxial nanofibers indicated the potentiality of these fibers over blended scaffolds [73]. Chen and his team developed a 3D-printed PLGA scaffold coated and loaded with dopamine and BMP2 & Ponericin G1, an antimicrobial peptide. Microscopic images depicted a pore size of the PLGA scaffold in the 468.9µm to 491.3µm. Besides, the scaffolds with and without dopamine coating have shown little or no significant changes in their compressive strengths (16.74Mpa). Further, the water contact angle of the scaffolds with and without dopamine coating was found to be 14.8° and 104.9°. The release profiles of growth factor and peptide were investigated, and the authors found that pure PLGA scaffolds released about 86.31% and 76.75% of BMP2 & Ponericin G1 in a day compared to dopamine-coated PLGA scaffolds, which released only 9.38% and 16.43% in 2 days suggesting a controlled release. Furthermore, MC3T3-E1 cells were loaded onto the scaffolds, and the cell production was performed by CCK-8 assay and observed a higher proliferation of cells on the scaffold coated with dopamine (~1.11 & 1.6) than that of pure PLGA scaffold (~0.75 & 1) on 4th and 7th days. Authors have also performed

qRT-PCR by selecting Runx2, OCN (osteocalcin), and OPN (osteopontin) and observed a rise in the appearance of OCN and OPN in MC3T3-E1 cells in modified scaffolds after 7 days compared to that of pure PLGA scaffolds [74].

5.3. Role of Growth Factors in Conjunction with Bioceramics for rapid bone healing

Zhang et al. developed a hierarchically salt-leached porous CSPC (calcium silicate (CS) /calcium phosphate cement scaffold (CPC)) loaded with recombinant human bone morphogenetic protein-2 (rhBMP-2) -CSPC/rhBMP-2. Results of the micro-CT scan depicted that CSPC scaffolds have a porosity of 70% and macro & micropores ranging from 200-500 µm and 2-5 µm. Furthermore, Rapid degradation of CSPC scaffolds (16%) was regulated by incorporating Calcium silicate (5%), suggesting deceleration in weight loss as reported by the authors. Release profiles of rh-BMP2 from the developed scaffolds have shown controlled release of GF from the CSPC (43.4%) scaffold compared to its contrast (60%). C2C12 cells are isolated on every type of scaffold. The outcomes of MTT, ALP (2-fold increase), and RT-PCR have validated the increased cell responses on CSPC/rh-BMP2 scaffolds compared to another set of scaffolds. Authors have also investigated the bioactivity of rhBMP-2 released from CSPC, free rhBMP-2 discharged from CSPC, and rhBMP-2 incubated with 70 ppm Si ions. They observed elevated ALP activity in cells mediated with rh-BMP2 released from CSPC and rh-BMP2 incubated with Si ions. Researchers have also analyzed ectopic bone formation in mice and observed the bone formation and some new blood vessels in the group of scaffolds with GF compared to pure scaffolds. Furthermore, they have also assessed bone regeneration capacities of scaffolds in rabbit femur cavity defects, and results depicted a 2-fold rise in bone volume in CSPC/rhBMP-2 compared to its counterpart [75]. In this study, Overman et al. studied the effect of BMP-2, scaffold matrix, and degree of differentiation on the number of proteins expressed by human adipose stem cells (hASCs). hASCs were isolated on tissue culture plastic and BCP (biphasic calcium phosphate).BCP has 90% porosity with a particle size of 500-1000µm and a pore size of 100-500µm. Interpretation of trophic factors by hASCs cultured on plastic and BCP was evaluated, and it was found that hASCs cultured on BCP have shown larger expression of ~20 genes. However, the expression of ~50 genes was decreased on BCP compared to plastic. BMP-2 treated hASCs showed upregulation of ~30 factors. 27 factors exhibited differential expression depending on the type of substrate and effect of BMP2, among which there are 6 factors belonging to the fibroblast growth factor family. Authors reported qPCR assay of osteogenic differentiation genes and growth factors (RUNX2, COL1A1, BMP6, INHBA, TGFB1 IGF1, FGF2, and FGF1), among which expression of COL1A1 and RUNX2 was enhanced by 4-fold. No inducing effect of BMP2 on TGFB1 or FGF2 expression was observed. Expression of INHBA, IGF-1, and FGF-1 was increased with the treatment of BMP-2. Activin-A production was enhanced in cells cultured on plastic in contrast to BCP. Similar multiplication of the potential of cells loaded on BCP and plastic was observed. ALP action was lower in cells isolated on plastic than BCP, and BMP-2 treated hASCs, as reported by Authors [76]. The developed scaffolds' porosity and pore size ranges were 60% and 100-400µm, respectively. Authors have cultured osteoblast-like cells- MG63 on developed scaffolds and stated that Sr doped scaffolds had shown better cell compatibility (viability and cell attachment) than undoped and control groups. The more VEGF and bFGF estimated by ELISA assay in Sr doped scaffolds were 364.989 pg/mL and 27.085 pg/mL, respectively, significantly higher than other scaffolds. Further, in-vivo studies conducted in rabbits have shown increased new bone formation in scaffolds with Sr doping and MSCs compared to scaffolds without MSCs, as reported by Gu and the team. In addition, the rate of new bone formation correlated with the degradation of developed scaffolds after 16 weeks of post-implantation [77]. Shangsi et al. plotted a Hydroxyapatite (a natural form of calcium apatite) porous scaffold loaded with vascular endothelial growth factor (VEGF) and morphogenetic protein-2(BMP-2) growth factor. Authors have reported a good adherence (pseudopodia-like structure formation) of seeded cells (rat MC3T3-E1) which covered the entire scaffold surface. Further, cell differentiation was maximum on scaffolds containing growth factors by observing the maximum expression of lineage-specific genes like OPN, Col-1, and ALP. After the implantation of scaffolds in the rabbit skull, they observed that Bone volume to tissue volume (BV/TV) and trabecular number (tb. N) were 2 folds greater in scaffolds containing growth factors in contrast to its counter. Furthermore, H and E staining images have depicted increased collagen –I and lectin on composite scaffolds compared to pure scaffolds suggesting compatibility of developed scaffolds for Bone tissue reconstruction [78]. Mijiritsky et al. prepared Hydroxyapatite (porcine origin) based scaffolds filled with mesenchymal stem cells (MSCs) for controlled release of vascular endothelial growth factor (VEGF) and basic fibroblast growth factor (bFGF) to increase bone tissue formation and vascularization by implanting into rat calvaria. Viability of seeded MSCs on different scaffolds (blank scaffold, scaffold with MSCs, scaffold after trypsinization, and scaffold with MSCs after decellularization) was performed by MTT, and the results showed a 2-fold increase in cell viability on scaffolds with decellularized MSCs in contrast to other scaffolds. Further, the results of osteogenic differentiation (Von Kossa and Alizarin Red Staining) have revealed a high rate of calcium deposition in the scaffolds with decellularized MSCs when compared to its counter. In addition, Mijiritsky and his team reported that Histomorphometric analysis (measurement of shape or form) of the scaffold with and without GF had shown new bone formation areas of 175 μm^2 and 145 μm^2, respectively. The results of real-time PCR suggested that scaffolds with decellularized MSCs had a 2 folds higher expression of RUNX2, Osteopontin, Osteocalcin, Collagen type 1, CD31, VWF markers, and discharge of VEGF when compared to native bone granules suggesting the role of GF s in bone TE [79]. Gonzalez et al. prepared SBF-coated beta-tricalcium phosphate porous scaffolds loaded with two growth factors, namely VEGF and mBMP-2. They studied the effect of coating on scaffolds to deliver GFs effectively. Further, authors have reported a direct role of Growth factors in neovascularization. They suggested that SBF Coating has increased the binding and releasing ability of GFs. The results of the GF release suggested that delivery of both VEGF and BMP was high (~2 times) in cell culture media compared to SBF, as reported by the authors. Histological studies revealed that profuse vasculature was noticed in scaffolds with VEGF (10 µg) and BMP (50µg), respectively, and no bone formation was noticed at varied concentrations of GFs [80]. Perez and his team developed SBG (silica-based bioactive glass) microcarriers. They incorporated it with cyt C (cytochrome C) and bFGF (basic fibroblast growth factor) to study the release profile of GF. The morphological analysis demonstrated that the microcarriers possessed a diameter of about 200 to 300µm. The release profile, when observed for cyt C and bFGF, depicted a release

of about 2% & ~5% in a week and ~11 to 14% and 20% in 5-6 weeks. Further, MSCs were loaded onto the microcarriers and detected that the spread of cells was 75 to 90% in 2-7 days in bFGF-loaded microcarriers compared to bFGF-free microcarriers was only about 30 to 55% [81].

5.4. Role of Growth Factors in Conjunction with Composite Biomaterials for rapid bone healing

Florczyk et al. has developed 3D porous β-TCP scaffolds in which Alginate gel was used to incorporate BMP-2 and to increase the cell seeding efficiency. It is the study in which the proliferation of MG-63 cells was studied on various types of supporting matrix, namely, pure β-TCP, β-TCP/Alginate, and β-TCP/Alginate/BMP-2. Authors reported an increased proliferation of seeded cells on β-TCP/Alginate and β-TCP/Alginate/BMP-2 porous scaffolds compared to the other two types of scaffolds. Further, 52% has been eluted from the Alginate matrix to porous scaffolds at day 13, with less than 5% in a day, suggesting a steady state release of BMP-2. In addition, results of Immunohistochemistry (confocal images) revealed an elevated level of Osteocalcin on scaffolds with Alginate and BMP-2 compared to its counterparts. Furthermore, increased blue color dots of explants after Masson's Trichrome assay suggest the deposition of collagen ad, thus, the formation of new tissue (osteoid) at the area of implantation, indicating the potentiality of Alginate gel-assisted porous β-TCP scaffolds loaded with BMP-2. The authors also reported that Alginate-assisted cell seeding had increased the uniformity of seeded cell distribution, leading to enhanced proliferation in both in vitro and in-vivo conditions [82]. In a study by Jun and his team, BMP-2 was entrapped in a silica xerogel chitosan (hybrid)-hydroxyapatite scaffold. In vitro and in-vivo studies were achieved by loading MC3T3 cells and implanting developed scaffolds in rabbit models, respectively. Spectroscopic results have shown a constant release of BMP-2 from HA scaffolds with silica xerogel chitosan loaded with BMP2 for up to 6 weeks. In contrast, HA/BMP2 scaffolds have shown burst release of GF, suggesting the significance of BMP 2 loading in xerogel. Further, Cell proliferation (MTS) results have shown 2-fold higher cell viability in hybrid-coated HA scaffolds than others. Hybrid-coated HA loaded with BMP-2 exhibited a higher level of cellular differentiation than pure HA scaffold, confirmed by ALP results as reported by the authors. Pure HA scaffold witnessed a lower bone regeneration level than BMP-2 loaded hybrid coated HA scaffold. 52% of bone formation was observed in BMP-2 coated hybrid scaffold, significantly higher than pure HA scaffold (24%) [83]. Yan su et al. prepared poly(L-lactide-co-caprolactone) (PACL)/collagen nanofibers loaded with Dex (Dexamethasone) and BMP2 (bone morphogenic protein) and assessed various physicochemical and biological applications of scaffolds. The addition of Collagen to PLACE has decreased the contact from 131 to 29°, suggesting increased hydrophilicity. Further, there is a slight decrease in compressive strength (3.96-3.79MPa) and fiber diameter (859-336 nm) of PLL ACL/Collagen fibers compared to virgin PLL ACL fibers. Further, BMP-2 and Dex were loaded into blended and core-shell scaffolds, and they compared the release of profiles. Release profiles of encapsulated drug and protein (BSA) were assessed in 3 stages (initial burst release, decrease release, and constant release) and were compared between various groups (mat A: blended PLLACL-collagen/DEX+BMP-2; mat B: core BMP-2; mat C: core BMP-2+DEX) and release percentages of DEX and BSA at stage-III from mats A, B, and C respectively are 70.8%, 81.1%; 74.9%,64.2%; 73.7%,60.5%. hMSCs (human mesenchymal stromal cells) were cultured and assessed for cell viability (MTS) and differentiation assays (ALP), and results depicted higher cell responses in growth factor-loaded nanofibers. Core-shell nanofibers showed higher expression of Osteocalcin compared to blended nanofibers [84]. A Pullulan-based nano gel was prepared by cross-linking (cholesteryl group- and acryloyl group) CHPOA with polyethylene glycol (PEG), which allows forced release of dual growth factors (BMP-2 and recombinant human FGF18) by Kobayashi et al. BMP2, FGF18, and PBS were incorporated into prepared hydrogels and implanted in these four groups ((CHPOA-PBS/hydrogel (group-I), CHPOA-FGF18/hydrogel (group-II), and CHPOA-BMP2/ hydrogel (group-III), CHPOA-BMP2+FGF18/hydrogel (group-IV) into skull bone defects of mice. μ-CT images have depicted more bone healing in hydrogels with one (BMP2) and two GFs (BMP2 and FGF18). Histological observations (by calcein and alizarin red staining at 8w & 0w, respectively) showed thick bone formation compared to the intact bone with abundant bone marrow in a dual growth factor hydrogel system. Authors also reported implantation of dual GF-containing hydrogel in Osx1-GFP: Cre/R26R mice resulted in the expression of Osterix1, suggesting the existence of osteoblast near the implanted site. Furthermore, defects treated with Group-IV (CHPOA-Rh-FGF18+ BMP2/hydrogel) have shown infiltrated osteoblasts, β-galactosidase-expressing cells, active bone healing, and induction of angiogenesis [85]. Chen et al. developed Rapid prototyped composite PLGA/TCP scaffolds loaded with BMP-2 and varied concentrations of icariin individually by either coating or incorporating. Micro-CT images of scaffolds have shown uniform shape with porosity and standard pore size of 75 ± 3.27% and 458 ± 25.6 μm, respectively. Degradation was less in scaffolds with higher doses of ICT than in other developed scaffolds. Compared to medium & higher doses of ICT, there was a significant decrease in compressive strength in scaffolds with lower doses of ICT, BMP2, and control. A controlled release of total BMP-2 content (31.24%) was observed in scaffolds coated with BMP-2. Furthermore, authors have also cultured bone marrow stem cells (BMSCs) isolated against rabbits for in vitro analysis of scaffolds. BMSCs cell attachment and ALP activity were higher in scaffolds incorporated/coated with ICT, and scaffolds plated with BMP-2 compared to BMP-2 incorporated scaffold and control. RT-PCR results have shown that m-RNA expression of Collagen-I and osteopontin was increased in BMP2 and ICT-coated scaffolds. Higher calcium deposition (4.3-fold) and mineralization in medium dosage of ICT-loaded scaffolds were observed, indicating the better osteogenic potential of ICT at a medium concentration (32mg) [86]. In this study, angiogenic factors (PDGF and VEGF) loaded (by electrospinning) freeze-dried SF (silk fibroin) /CaP (Calcium phosphate) scaffold were developed by Farokhi and his team. In addition, PLGA was electrospun on its surface to control the release of GF's. The porosity (SEM) of pure SF/CaP substrate was reduced from 70% to 30% when PLGA nanofibers were electrospun on its surface. Release kinetics of PDGF and VEGF, when loaded individually or coloaded into SF/CaP substrate, showed similar profiles of sustained release up to 28 days, and PDGF showed slower release compared to VEGF. Human umbilical vein endothelial cells (HUVECs)and HGF (Human gingival fibroblast) are used to determine the bioactivity of released PDGF and VEGF (observed bioactivity -80%, 85%). Furthermore, human osteoblast cells were cultured to assess the scaffold's biocompatibility. MTT and ALP assays were performed to check out cell attachment and differentiation, which showed increased cell responses in angiogenic factors

loaded scaffold. Authors have also performed in vivo studies in rabbits and reported that bone defects filled with angiogenic factors loaded scaffold showed bone formation along with some blood capillaries [87]. Vitor et al. produced a 3D hybrid PDLLA (poly (D, L-lactic acid)) scaffolds incorporated with chitosan-chondroitin sulfate nanoparticles (CH/CS NPs) loaded with platelet lysate-PL (PDLLA/CH/CS/PL). The authors reported that the pore size and porosity (SEM) of the hybrid scaffolds are 400 μm and 56%, respectively. In-vitro GF release profiles of PDGF-BB, TGF-β1, and VEGF were assessed, and the PDGF concentration was higher than the other 2 types of GFs. hASCs cultured on developed scaffolds have shown an elevated cellular response on scaffolds with GF's compared to their counterparts. As ALP is a previous osteogenic gene, the expression of ALP until day 14 was higher in PL-loaded scaffolds. The calcium content (Alizarin red staining) was also significantly higher in PL-loaded scaffolds compared to non-loaded ones. Expression of a few other osteogenic markers like Runx2 and Osteocalcin was over-expressed for PL-loaded scaffolds compared with control scaffolds [88]. Hongxu et al. developed a collagen/PLGA scaffold in which BMP-4 was entrapped using a specific fusion protein-CBD (collagen binding domain extracted from fibronectin). Authors have reported an increased entrapment of BMP4 in scaffolds with an increase in the concentration of CBD. Affinity and adherence of the fusion protein to the collagen/PLGA hybrid scaffold were evaluated. Higher doses of CBD-BMP4 showed higher adherence to the collagen-PLGA hybrid scaffold compared to wild-type BMP-4. MSCs were grown in all the scaffold groups (BMP 4 coated and uncoated), and the results of in-vitro experiments have proposed an increase in cell responses on CBD-BMP4 containing scaffolds as compared to wild type for the predetermined period of 24 hrs. Furthermore, the cell-scaffold construct was implanted subcutaneously in mice. Post-implantation results have revealed elevated levels of ALP, suggesting that the scaffolds are suitable for osteogenic differentiation of MSCs in an animal model. Along with positive results of Von-Kassa (calcium deposition) and increased expression levels of C1, SPP1, OC in CBD-BMP4 immobilized collagen/PLGA scaffold suggesting the ability of CBD coated BMP4 scaffolds for BTE [89]. Dong et al. developed the coaxial electro-dropping method of PLGA-alginate microcapsules with core-shell microstructure. Microcapsules were encapsulated with BMP-2 and Dex by altering their positions in core and shell domains. Micrographic images have shown wrinkled and rough surfaces of microcapsules. The average size of microcapsules was 400-500μm, as reported by the authors. Release profiles were determined using a UV spectrophotometer and ELISA for Dex and BMP-2. Irrespective of its location, no initial burst was noticed in the case of Dex, whereas BMP-2 has shown an initial slow burst at both the core and shell. Authors have also reported increased cell viability (trypan blue dye exclusion test) and differentiation ability (type I collagen, Osteocalcin (OC), and osteopontin (OP)) of rat BMSCs on alginate hydrogel scaffolds loaded with microcapsules containing GF as compared to wild. were loaded into alginate hydrogel in addition to growth factor-loaded microcapsules [90]. Pengfei et al. established a composite scaffold using Gelatin, chitosan, and varied concentrations of polyvinyl alcohol (1%, 6%, 12%, 18%) and nanohydroxyapatite (0.75%, 3%, 12.5%, 50%). Polyvinyl alcohol improved the mechanical strength of the scaffold. Still, a further increase in its concentration (12%, 18%) resulted in a decrease in porosity, pH value, increased compactness of the scaffold, and a faster degradation rate. Hence, a 4:4:12 ratio of Ge: CS: PVA was selected to incorporate varied concentrations of Hydroxyapatite. Similar changes w.r.t PVA were observed with an increase in the concentration of Hydroxyapatite, suggesting a controlled concentration of Hydroxyapatite is suitable for bone regeneration. Furthermore, authors have also cultured rat bone marrow stem cells on advanced scaffolds to assess the osteogenic-inducing ability of the scaffolds. Cell viability, osteogenic differentiation (ALP assay), mineralization (Alizarin red staining), and expression of osteogenic markers like RUNX2, ALP, OCN, OSX, BMP2, and OPG (q-PCR) were higher on scaffolds with 12.5% & 50% concentrated hydroxyapatite. Authors have suggested 12.5% concentrated Hydroxyapatite as optimal for bone tissue regeneration [91]. Khojasteh et al. prepared (b-TCP) beta-tricalcium phosphate scaffold coated with (PLGA) poly lactic co glycolic acid filled with endothelial growth factor (VEGF) using Polyurethane foam casting method and cultured (cMSCs) canine mesenchymal stem cells and (cEPCs) canine endothelial progenitor cells. The compressive strength of β-TCP and β-TCP/PLGA scaffolds was 0.42 and 6.62MPa, respectively. Authors have reported an increase in the release of VEGF (6.87ng/ml to 165.92 ng/ml) with an increase in the growth factor concentration (0.1 -3 μg). Viability (MTT) and proliferation of seeded cells were high on TCP/PLGA scaffolds loaded with VEGF compared to pure TCP and TCP devoid of GF. Furthermore, using real-time PCR analysis, Khojasteh, and his team validated the raised expression levels of various markers like COL1and RUNX2, Von Willebrand factor (VWF-blood clotting gene), and Vascular endothelial growth factor receptor genes (VEGFR2) on β-TCP/PLGA/VEGF scaffolds when compared to β-TCP/PLGA scaffolds [92]. Bastami and his team prepared a highly porous 3-dimensional β-tricalcium-phosphate scaffold coated with Gelatin with 2 perpendicular canals filled with collagen hydrogel evenly spread on chitosan (CS) nanoparticles loaded with BMP-2 by using the Polyurethane foam casting method and delivered VEGF to human buccal fat pad-derived stem cells (hBFPSCs). The porosity of β-TCP/gelatin and β-TCP scaffold is 70.6% and 97.7%, respectively. After coating with a gelatin layer, strength significantly increased from 0.31MP to 1.21MP. The best biodegradation was observed in the β-TCP/gelatin scaffold when compared to the β-TCP scaffold. rhBMP2 release decreases up to 42% as time increases. Cell proliferation on the β-TCP/gelatin/rhBMP2 scaffold is slow compared to the β-TCP/gelatin scaffold. Moreover, 0.147mg/ml and 0.245mg/ml of ALP activity were observed, respectively [93]. Sobhani et al. prepared calcium phosphate and polyphosphazene composite scaffolds incorporated with BMP2 entrapped in Chitosan microspheres - CaP/PDMAP/CM/BMP-2. Cell viability (bone marrow stromal cells) by MTT assay showed the nontoxic behavior of prepared scaffolds. Results of Western blotting have shown higher expression of osteonectin (ON) and osteopontin (OPN) on CaP/PDMAP/CM/BMP-2 scaffold as compared to its counterpart (Without GF), suggesting an increase in osteogenic differentiation. Further, microscopic images (SEM) revealed that seeded cells adhered by covering the entire scaffold surface indicating good biocompatibility of developed scaffolds. In addition, Sobhani and the team evaluated protein expression. They reported elevated levels of expression by bone marrow stromal cells from 1.3 to 3.2 times greater in CaP/P-1/CMs10 and 2.1 to 4.1 times higher in CaP/P-1/CMs30 by the end of 14 to 32 days [94]. Lei et al. prepared chitosan scaffolds containing various strontium ion concentrations (1, 5, 10), which are incorporated into Hydroxyapatite (SrHAP/CS) by freeze drying method, which caused increased

cell proliferation of human bone marrow mesenchymal stem cells (hBMSCs). The presence of sr+2 ions in the SrHAP/CS scaffold showed more biocompatibility and osteoinductivity within 3 to 7 days when analyzed using CCK-8 assay, along with high ALP activity compared to HAP/CS scaffold as reported by Lei and team. The SEM studies have shown a pore size range of 100 um to 400 um, which assisted in the development of new blood vessels and nutrient channels that helped in the growth of cells and bone tissue. By the q RT-PCR assay and Western blotting results, authors have observed that RUNX2, COL-I, and ALP gene expression is high in Sr10HAP/CS compared to its contrast due to the presence of more concentration of Sr+2 ions in 10% Sr in composite scaffolds [95]. Lin et al. used stereolithographic technology (VL-PSL). They developed lentiviral (Lv) constructs possessing green fluorescent protein (GFP) and bone morphogenetic protein-2(BMP-2) on one scaffold (BMP group) and green fluorescent protein gene (Lv-GFP) alone on another scaffold (GFP group). Human bone marrow-derived mesenchymal stem cells (hBMSCs) were grown, and reported that the BMP group showed an enhanced cellular response over its GFP group as they released greater BMP-2 protein. Using the ELISA method, they studied that BMP-2 secretion is 2 folds higher in the BMP group. High ALP activity is found in the BMP group, which is noticed by thick purple coloration on the entire scaffold. Through the RT-PCR method, they studied the expression of biomarkers. They showed that the interpretation of RUNX2, COL-1, OCN, and BSP II is 2 folds higher in the BMP group, resulting in significant cell differentiation into osteocytes. Lin and team incorporated 2 scaffolds into 2 hindlimb musculature of mice and, through µ-CT images, interpreted that the BMP group scaffold has a total calcium content of 3.6 µg and mechanical strength of 350KPa, whereas the GFP group scaffold with a total calcium content of 0.08µg and mechanical strength of 35KPa. Hence BMP group scaffolds are more optimal than GFP group scaffolds [96]. Gentile and the team prepared a porous chitosan gelatin (CH/G) scaffold loaded with simvastatin (increases bone mineral density) incorporated in PLGA microparticles (CH/G/PLGA-S). Results of SEM images revealed an increase in the pore size from 100-300µm with a rise in the concentration of PLGA from 3.33 to 16.6 and 33.3%w/w. The mechanical stability of the scaffold raised from 2 to 4 folds as the concentration of PLGA increased from 3.33 to 16.66%w/w, however further raises in the concentration of PLGA gradually decreased the mechanical strength from 23 kPa to 9.8 kPa and swelling rate upto 3 folds and authors reported an optimal concentration of PLGA as 16.6% w/w. In addition, the authors also reported that hFOB (clonal human osteoblastic) cell proliferation is highest in scaffold CH/G/PLGA-S. Simvastatin release was 70% in scaffolds with a PLGA concentration of 16.6 compared to scaffolds with other weight content of PLGA. Furthermore, loaded cells' viability and osteogenic differentiation potential (ALP expression) were 2 and 3-fold higher, respectively, on CH/G/PLGA-S as compared with CH/G [97]. Yu et al. prepared a heparan sulfate layered perlecan domain 1(PlnD1) bounded poly e-caprolactone (PCL) scaffold and compared it with PlnD1 free PCL scaffold to study the constant discharge of recombinant human bone morphogenetic protein-2(rh BMP-2). Yu-Chieh and the group used radioactive labeling technology and concluded that PlnD1 bounded PCL scaffold had a 4-fold higher loading capacity when compared to the pure PCL scaffold. Yu-Chieh and co-cultured W20-17 mouse bone marrow stromal cells on PlnD1/PCL scaffold and pure PCL scaffold and noted that a 1-fold higher amount of ALP expression by rhBMP-2 was observed in scaffold with PlnD1. Within 23 days, 45ng/scaffold of bioactive rhBMP-2 is discharged from PlnD1- PCL scaffold, and only 32 ng/scaffold discharged from PCL scaffold, indicating that high and controlled release is achieved by PCL scaffold with PlnD1 [98]. Somying and team prepared a β-tricalcium phosphate (TCP) scaffold attached with hydrolyzed polymer containing collagen peptide (HPBSu/TCP) and a b-tricalcium phosphate (TCP) scaffold containing pure collagen peptide (PBSu/TCP) with the help of supercritical CO_2 technique which is later tagged with red fluorescence(5-TAMARA) and cultured human mesenchymal stem cells (hMSCs). SEM results showed that HPBSu/TCP scaffold has more pore size (514.91 µm) when compared to PBSu/TCP scaffolds (469 µm). The emission of fluorescence dye was observed in the HPBSu/TCP scaffold with peptide, which resulted in a clear and intense image with red coloration, indicating well immobilization of peptides on the scaffold compared to its contrast. Micro -CT scanning analysis revealed that large pores in the outermost layer of scaffolds have increased mechanical strength. Micro graphical images displayed the various stages of MSCs cultured till 21 days. The results showed that, on day 1, cells on HPBSu/TCP scaffold could form extensions like filopodia and lamellipodia, which assisted cells in penetration. Further, the formation of bridge-like and star-shaped structures on days 3 and 7 indicated the presence of a high number of cells and, thus, proliferation, respectively. At the end of day 7, the cells were observed to be evenly spread throughout the scaffold containing peptide resulting in better cell proliferation when compared to scaffolds without collagen peptide [99]. Xingyu and team prepared poly (lactide-co-glycolide)/hydroxyapatite (PLGA/HA) fibrous scaffold, which is plated with polydopamine (PDA) (PDA-PLGA/HA) loaded with BMP-2. The presence of HA raised the hydrophilicity and surface roughness of pure PLGA scaffolds and favored better cell (MC3T3-E1) adherence. Further hydrophilicity is much improved in PDA-coated scaffolds. Results of ELSA showed that PDA-PLGA/HA scaffold could load 2-fold increased content of growth factor when compared to its counter. In addition, the PDA plating improved cell proliferation and differentiation of the scaffold, which leads to rapid bone formation in the PDA-PLGA/HA scaffold, as suggested by the authors. MTT (viability) and ALP (differentiation) were much better in PDA-PLGA/HA scaffold than PLGA/HA scaffold. Furthermore, expression of RUNX2 by 2 folds and increased mineralization in PDA-PLGA/HA/BMP-2 scaffolds has been attributed to Ca+ ion deposition by PDA compared to scaffolds without PDA [100]. Lingyan et al. prepared polycaprolactone fibrous scaffolds filled with BMP-2 using 2-N, 6-O-sulfate chitosan (PCL-N-S) and studied the impact of Sulfate concentration on fiber diameter and hydrophilicity. Authors have reported a 2-fold increase in the parameters mentioned above as the concentration of Sulfate increased. Furthermore, results of ELISA have shown PCL, PCL-N/0.6 - S, and PCL-N/1.2-S scaffolds have BMP-2 loading capacities of 1000, 2000, and 6000pg, respectively. With a rise in the concentration of Sulfate, the scaffolds have released BMP2 Sustainably; 1.2 S has released only 10 % of loaded GF In the first 5 hrs, whereas others have released 30%. In addition, researchers have cultured bone marrow mesenchymal stem cells (BMSCs) on all 3 groups of scaffolds. The outcomes have indicated a 12 times higher rate of proliferation and differentiation on the PCL-N/1.2-S scaffold compared to its counter, indicating the suitability of developed scaffolds in controlled growth factor distribution and, thus, in bone tissue engineering [101]. Hao-Xuan and the group prepared a calcium

phosphate composite scaffold filled with VEGF and BMP incorporated in the PLGA microsphere (VEGF/BMP-PLGA-CPC). No significant difference exists in the physicochemical and mechanical properties of scaffolds observed by incorporating GFs. The osteogenic differentiation of Bone marrow mesenchymal stem cells (BMSCs) and viability using CCK8 and ALP assay has suggested increased viability and differentiation on scaffolds possessing both GFs compared to scaffolds with single GF and without any GF. Further, authors have reported the expression of CD31 using histochemical analysis suggesting differentiation of MSCs to epithelial origin cells. The team also performed In-vivo studies by implanting various scaffold groups into rabbits with ANFH (A type of bone tissue death). Post implantation (micro-CT images) have depicted 86% of bone formation along with 211.4mg/cm^3 of bone mineral density (BMD) on scaffolds with BMP and VEGF, whereas scaffolds with one and no growth factor have shown less BMD. Furthermore, H&E staining images after 12 weeks have shown intense coloration suggesting rapid new blood vessel formation in the BMP-VEGF-PLGA-CPC scaffold in contrast to its counterpart suggesting the role of growth factors in healing ANFH [102]. Bae and the team prepared AEMA cross-linked Hyaluronic acid/Heparin hydrogels loaded with BMP2. Authors have compared the mechanical stability of prepared hydrogels (HA gel, 0.5mg/ml of heparin-implanted HA hydrogel [HA + Lhep gel, 1 mg/ml of heparin-implanted HA hydrogel [HA+Hhep gel, 0.5mg/ml of heparin-AEMA implanted HA-AEMA hydrogel [HA-g-Lhep gel and 1mg/ml of heparin-coated AEMA implanted HA coated AEME hydrogel [HA-g-Hhep gel) with HA/AEMA gels. They reported that there is no significant difference in compressibility and swelling. The growth factor release from hydrogel is slow and controlled in 1mg/ml of heparin-coated AEMA implanted HA-coated AEME hydrogel (HA-g-Hhep gel) compared to its counter. There is no considerable difference in the hydrogels' cell viability. However, HA-g-Lhep gel showed 103% of cell viability. Furthermore, ALP assay results fluctuated for all the scaffolds, but the scaffolds with BMP-2 showed an increased expression of ALP [103]. Quinlan et al. has developed rhBMP-2 incorporated Collagen-Hydroxyapatite (CHA) composite scaffolds with a pore size and porosity of 75µm and 96% correspondingly using Freeze drying. Growth factors were encapsulated in a polymeric matrix of Alginate and PLGA microparticles (1-10µm) which were prepared by spray drying and double emulsion techniques. Authors reported that binding efficiency and discharge of BMP-2 in Alginate and PLGA are 45%, 83%, 46%, and 12%, respectively, indicating an increased release of BMP-2 from Alginate in contrast to PLGA microparticles. Further, Alginate and PLGA microparticles, including BMP-2, were incorporated into CHA composite scaffolds to check the rhBMP-2 release. The results state an increased osteogenic response (ALP expression) was noticed on BMP-2 releasing PLGA-CHA scaffolds compared to its counterpart. Furthermore, in-vivo results of histological analysis have confirmed the growth of new bone in the entire defect area with BMP-2 eluting PLGA-CHA. On the other hand, newly formed bone was limited to only edges of the bone defect, suggesting an accelerated bone healing in scaffolds with BMP-2 compared to scaffolds without any GFs [104]. Zheng and his team prepared PLGA-nHA composite coated with PLGA-PEG-PLGA hydrogel entrapped with PRF-derived growth factor 9(platelet-derived growth factor-AB (PDGF-AB), transforming growth factor- 1 (TGF- 1) and insulin-like growth factor-I (IGF-I)). Microscopic images have depicted pores with a size of 70-160µm. Authors have reported a burst release of IGF-1, TGF-B1, and PDGF growth factors for the first 24hrs and a controlled release after 3 days. The increased release rate of TGF-B1(36.2%) was greater when compared to IGF-1(34.2 %) followed by PDGF-AB (32.9%,). However, after 4 weeks, the release rate is almost the same for IGF-I (66.29%) and TGF-1 (66.8%,) as reported by the authors indicating the continuous release of loaded GFs. nHA/PLGA/Gel-PRF seeded with MG63 cells showed good cell viability (CCK-8) and proliferation (CCK-8) compared to the scaffold without growth factors. In addition, cell spreading and attachment was also high on scaffolds with GFs compared to their counterpart advising the part of GF in bone Tissue Engineering as denoted by the authors [105]. Wang et al. fabricated BCP (biphasic calcium phosphate) scaffold with Chitosan/Chondroitin sulfate nanoparticles (NP) containing BMP-2 (3.05ng/cm2). As reported by the authors, the pore size, porosity, compressive strength, and surface area of prepared scaffolds are 50-500µm, 81%, 2.22Mpa, and 0.59 cm2/g, respectively. Release of GF from the scaffolds with nanoparticles was slow (36.9%) and sustained compared to scaffolds without nanoparticles (71.6%), indicating the significance of nanoparticles in GF release kinetics. Further, authors have noticed a high proliferation (Alamar blue test) and ALP activity of BMSC on BCP with nanoparticles compared to other scaffolds such as BCP and BCP/NP/dopa. In addition, a 14-fold increase in OID Value was observed, suggesting an abundant deposition of collagen type-1 on BCP/NP followed by BCP/NP/Dopa and BCP [106]. Xiaoning et al. developed BMP-2 releasing chitosan/alginate/hydroxyapatite scaffold (C-Ag-HA) with a pore size and porosity of 100-110µm and 74.5% by co-precipitation and solvent sublimation method. Authors identified controlled and continuous discharge of BMP-2 from the C-Ag-HA/BMP-2 scaffold (64%) when contrasted to Collagen/BMP-2 (84%) scaffold. Good biocompatibility with no cytotoxicity (MTT assay) was observed on C-Ag-HA/BMP-2 when seeded with MSCs. Differentiation assays like ALP, Alizarin red staining, and qRt-PCR indicated MSCs were well differentiated due to the expression of various markers like OCN, Col I, and OPN. Further, the authors reported that biomineralization was 2.7 times greater in C-Ag-HA with growth factors and cells when compared to control (C-Ag-HA). Among all these scaffolds, C-Ag-HA /BMP-2/MSC construct has shown a higher bone mineral density (0.22g/cm2) and neo bone formation [107]. Jiabing et al. developed BMP-2 releasing 3D porous Chitosan chondroitin sulfate scaffold (CH/CS) with 100-150 micrometer pore size. The release of GF from coated(apatite) scaffold Was nearly 2 times smaller compared to non-coated scaffolds indicating the continuous release due to greater interactions between growth factor and apatite coating. Adipose-derived stem cells have been grown on prepared scaffolds. The results have shown high cellular responses such as adherence (microscopic images) and proliferation (Live and dead, Alamar blue assay) on BMP-2-containing apatite-coated scaffolds compared to its counterpart. Further, authors have also stated a rise in the higher appearance of collagen (6 folds) and OCN (2 folds) on coated scaffolds with GF compared to pure scaffolds. Furthermore, the amount of new bone formation and BT/VT was 50 and 45% high when GF-loaded scaffolds were implanted in rats to observe bone regeneration [108]. Sheehy developed Chitosan/HAp composite scaffolds and studied the effect of PGF using various entrapment techniques. Controlled release of GF was observed from scaffolds with a combination of microparticles and direct loading compared to individual loading scaffolds. A higher degree of cell adhesion (SEM images) was reported in GF-entrapped scaffolds when seeded with HUVEC. Furthermore, higher DNA content(qPCR) and

Calcium deposition were noticed on scaffolds with GF compared to pure scaffolds. In addition, scaffolds with GF have shown more ALP activity, suggesting PGF-loaded scaffolds' osteogenic potential. Scaffolds were implanted subcutaneously in rat calvaria defects. The outcomes of Micro-CT and H&E staining images have suggested abundant bone formation in GF entrapped in dual-way scaffolds compared to the other type of scaffold. In addition, results of Immunofluorescence have depicted the expression of CD31 (angiogenesis marker) in GF-loaded scaffolds, indicating the occurrence of new blood vessels at the site of implantation, as reported by the authors [109]. Wang et al. prepared Chitosan-Genipin scaffolds coated with nanohydroxyapatite and loaded with BMP-2. It was stated that the loading capacity of bmp-2 in coated and uncoated scaffolds was 65 and 28%, respectively. Slow and controlled release of bmp-2 was observed in coated scaffolds (55%-Day3) compared to its counter (28%-day3). The continuous release of bmp-2 coated scaffold was due to the connections among functional groups of BMP-2 and nHAp.CLSM images depicted a good cellular response on coated scaffolds with growth factor when seeded with BMSCs compared to the counter. ALP assay and Rt-PCR results have shown a raised appearance of osteogenic markers like ALP,runx2, OCN, and OPN were 4, 2.4, 7, and 2.8 folds greater on coated scaffolds than uncoated, indicating the potentiality of developed scaffolds towards BTE.Furthermore, elevated levels of cbfa1 expression suggested the suitability of scaffold matrix for seeded cell differentiation into osteocytes, as reported by the authors [110]. Zhang developed BMP-2 entrapped gelatin-coated 3D porous PCL scaffold for curing bone defects. As Gelatin concentration varied from 5%-20%, authors observed a decrease in porosity & swelling whereas an increase in mechanical strength. Authors have optimized the gelatin concentration for effective coating and release of rh-BMP2 and stated that 5 and 10% were ideal for studying the in-vitro cell responses. Precise discharge of rhBMP-2 was reported in scaffolds coated with 5%gelatin (decreased 1900, 138, 682,300ng) compared to scaffolds without any gelatin coating. HMSCs were seeded on coated and uncoated scaffolds. The results of MTT, Calcium deposition, and ALP have shown that scaffolds with 5% gelatin coating loaded with BMP2 had higher cellular responses than other types. Further, subcutaneous implantation was done in mice. Histological studies revealed uniformly distributed new bone formation on the scaffold (5%gelatin) loaded with GFs compared to its counterpart, signifying the part of GF in bone tissue regeneration as suggested by the authors [111]. Senator et al. prepared growth factor (BMP-2) loaded (polyethylene-hydroxyapatite (UHMWP)) and polyether-ether ketone-hydroxyapatite (PEEK) scaffolds. They reported an enhanced release (22%) of bmp-2 from (the polyethylene-hydroxyapatite) scaffold as compared to others (12%) in 10 days. Two sets of scaffolds were implanted in the cranial defect site of mice, and found 12,2-, and a 2-fold increase in elastic modulus, BV/TV, and Maximum load ratio was observed on BMP-2 loaded polyethylene-hydroxyapatite (22, 12.18, 24) scaffold when compared to the scaffold without growth factor (2.36,1.33, 12). Similarly, authors have also reported an increase in elastic modulus, BV/TV, and Maximum load ratio properties on polyetheretherketone-hydroxyapatite scaffolds with GF (6.83, 16.44, 6.20) as compared to free scaffolds (4.04, 9.13, 0.41) and overall indicating good mechanical strength of polyethylene-hydroxyapatite/BMP-2 scaffold compared to another type of scaffold. The histological analysis reported that scaffolds with GF have shown more bone volume, collagen fibril deposition, and bone area than its counterpart, indicating the potentiality of developed scaffolds using GF [112]. Kang et al. prepared PLGA-PEG-COOH (VEGF-FGF), and Gelatin microparticles (BMP-2) incorporated nHA-PLGA composite scaffolds using CO_2 foaming technology. The release of VEGF (49.65%) was greater compared to FGF-2 (48.24%) and BMP-2 (14.7%), which are attributed to angiogenesis followed by osteogenesis. BMSCs were seeded; increased proliferation (CCK8) and expression of ALP, OCN, and Col-1 were observed on scaffolds with microparticles containing GFs compared to scaffolds with free GFs. Micro CT and histological analysis showed that the prepared novel scaffold had increased BV/TV and BMD from 35%& 0.74g/cm3 to 46.92%, & 0.91 g/cm3 indicating ectopic bone formation. Expression of CD31+ cells was noticed, indicating new blood vessel formation when implanted in rats subcutaneously [113]. Zeynep Bal Developed novel PLA-PEGC (5mg)-nHAp (12.5mg) (polylactic acid−polyethylene glycol, nano-hydroxyapatite) scaffolds for controlled discharge of BMP-2 aiding in osteoinduction. The discharge kinetics of BMP-2 displays that burst early discharge (3%) followed by controlled release (6%) over 21 days. Two concentrations of BMP-2 (3&10µg) were used to assess new bone formation when implanted in rats. Though similarities were observed in PLA-PEG C/nHAp with different concentrations of GFs, there are certain differences concerning Bone volume (60), trabecular volume (75), and BV/TV (85), and the scaffolds with 10 micrograms have shown increased values when compared to its counterpart. H&E and Safranin O staining images indicated that profuse osseous was detected in the presence of BMP-2, as reported by the authors [114]. Xiangjun et al. prepared PLGA (Poly (Lactide-co-glycolic Acid)) immobilized with 26SCS (2-N,6-O sulfated chitosan) for controlled delivery of growth factor(rhBMP-2). Different concentrations of PLGA ranging from (0.05, 0.1, and 0.2 mol/L) were taken to study release kinetics and cellular responses. SEM images indicated a rough morphology on A-PLGA 0.2. Perfect incorporation of 26SCS onto PLGA (0.2) scaffold can be confirmed by Ninhydrin (deep purple) and TB staining(purple). Lower initial burst release and higher binding efficiency of A-PLGA 0.2 cause steady and controlled discharge of rhBMP-2 compared to other scaffolds. A decreased water contact angle was reported on S-PLGA, indicating an increased hydrophilic nature and greater cellular responses when seeded with C2C12. ALP activity was increased by 2 folds compared to other groups of scaffolds, indicating the suitability of developed scaffolds for differentiation of C2C12 on S- PLGA scaffolds with 0.2mol/L [115]. By freeze-drying, Ciara developed bmp2 and ZA (zoledronic acid) enriched collagen hydroxyapatite (CHA). Despite the addition of Zoledronic acid, there was no significant change in cell viability when they used MC3T3E1 cells. Varied concentrations of ZA(5-10ug) and BMP-2(5-10ug) were used to prepare composite scaffolds implanted subcutaneously in the rat's hind limb. Higher amounts of bone formation were noticed on the 10 ug ZA/10ugBMP-2/CHA scaffold compared to other concentrations. further, there is a significant reduction in osteoclast number, suggesting the change in bone metabolism leading to fast bone growth on 10 ug ZA/10ugBMP-2/CHA scaffold (59).Hana and his team prepared hydroxyapatite (HA) scaffolds coated with Poly (L-lysine) (PLL)/ Polydopamine (PDA) followed by entrapping BMP-2 and observed the discharge pattern of BMP-2. Researchers prepared and categorized scaffolds into three groups: HA, HA/BMP-2, and HA/PLL/PDA/BMP-2, and reported that pore sizes greater than 150µm have been shown to promote internal mineralized bone growth. Furthermore, the authors reported that the mechanical stability and porosity

of pure HA scaffold were 1.7 ± 0.2 MPa and 66.5%, respectively. Furthermore, BMSCs were loaded on prepared scaffolds. The outcomes suggested an increase in cell viability was observed by MTT assay. CLSM images suggested greater cell attachment on HA/PLL/PDA/BMP-2 compared to the other scaffold groups. Masson's trichrome staining has depicted an elevated level of mineral deposition in the newly formed bone tissue at the implantation site. Thus, the authors reported the benefit of adding BMP-2 to HA scaffolds has not only increased in vitro cell responses but also in vivo [116]. Thomas and his team prepared alginate-based composite scaffolds by loading various glass-ceramic (GC) concentrations by Freeze drying. Morphological analysis of prepared scaffolds revealed porous architecture with a pore size between 110-380 µm, and authors also reported a reduction in pore size with the rise in ceramic content. Further, the porosity of the alginate scaffold was constituted to be 88%, whereas counterparts have shown 82-85%. Moreover, it was also studied that an increase in GC content increased the mechanical stability of the scaffolds, the highest being 0.7 MPa at GC3 concentration. Furthermore, MG-63 cells were used to study the cell viability by MTT assay, and the outcomes presented that both the scaffolds displayed a higher cell proliferation, and among the composite scaffold, GC3 displayed a higher cell proliferation. Besides, ALP activity was also recorded, and it was found that increasing GC content increased ALP activity to ~2 folds. Additionally, in vitro mineralization using Alizarin Red S (ARS) staining suggested higher mineralization in alginate-GC scaffolds compared to alginate scaffolds, which promoted osteoblast expression and extracellular matrix deposition [117]. Hu and team prepared nanohydroxyapatite (nHAP)-collagen (COL) scaffolds which were further incorporated with bFGF and BMP2. From SEM images, the scaffolds' pore size and thickness were found to be in the range of 80-200µm and 1-2µm. The cumulative release of bFGF from nano hydroxyapatite-collagen and BMP2 from nano hydroxyapatite-collagen was measured to be 91% and 90%. The adhesion rate of BMSCs on the nano hydroxyapatite-collagen scaffold with dual growth factors was higher (~98%) compared to the scaffolds containing a single growth factor (~90%) as scaffolds without any growth factor. (~80%). Furthermore, in 7 days, the proliferation of BMSC cells on the scaffolds containing both the growth factors and bFGF-loaded nano hydroxyapatite-collagen scaffolds were found to be comparatively higher (~2 and 2.1) than the pure nano hydroxyapatite-collagen scaffold and BMP2 embedded scaffold (~1.7 and 1.9). It was also noted that dual growth factors containing nano hydroxyapatite-collagen scaffolds displayed an increase in differentiation (ALP activity) of BMSC cells in contrast to other groups of scaffolds [118]. Wei and his team developed a bioink using SF (silk fibroin)/ GEL (Gelatin)/ HA (hyaluronic acid)/ TCP (tricalcium phosphate). They printed a 3D scaffold coated with human platelet-rich plasma (PRP) containing multiple growth factors. hADMSC (human adipose-derived mesenchymal stem cells) cells were seeded onto the scaffolds. By performing an MTT assay, they found that the cell proliferation and growth were much higher on the scaffold coated with PRP compared to the non-coated scaffold. Researchers have observed a considerable difference in the differentiation rate of seeded cells on PRP-coated and uncoated scaffolds. RT-PCR results have validated the osteogenic differentiation ability of cells by the enhanced appearance of markers such as ALP, RunX2, OCN, and OPN on scaffolds with multiple growth factors compared to its counterpart [119]. Udomlucka and his team fabricated nanofibers using Gelatin coated with HAp (Hydroxyapatite), which was further loaded with bone morphogenetic protein -2 (BMP-2) and fibroblast growth factor-2 (FGF-2) followed by SBF immersion. SEM images of nanofibers with and without SBF treatment have depicted fiber diameter and swelling ratios of 660-1380 nm and 650-196%, respectively. In order to examine cell production on gelatin nanofibers and HAp/gelatin nanofibers, hASC (human adipose-derived stem cells) cells were loaded onto the scaffolds with and without growth factors (FGF2/BMP2) and observed that HAp-coated gelatin nanofibers with growth factors had the highest proliferation rate and a 7-fold increase compared to the counterpart which showed a 3-fold increase. q-PCR was performed for all the 3 types of nanofibers and assessed the appearance of three osteogenic genes such as RunX2, COL1α1, and OCN, and found that this three gene expression was higher in the nanofibers coated with HAp as well as with growth factors compared to the nanofibers without coating and growth factor free scaffolds [120]. Yilgor and his team prepared chitosan and chitosan/PEO (poly (ethylene oxide)) blends. Further, these scaffolds were embedded with PLGA and PHBV nanocapsules loaded with BMP2 and BMP7, respectively, and obtained a porosity of 85%. Rat bone marrow MSCs were loaded onto the scaffolds, and observed that production and differentiation of seeded MSCs on chitosan/PEO blends showed increased responses as compared to pure CS scaffolds. Also, ALP activity on day 21 was higher in the PEO composite scaffold (1.3) than in the PEO-free scaffold (1.1). Authors reported that PLGA nanoparticles incorporated into the fibers significantly enhanced the release of BSA protein (95%) compared to PLGA incorporated into the fibers (70%) as well as PHBV nanoparticles (45-50%). Authors have reported enhanced cell proliferation (Alamar blue assay) and differentiation (ALP) on fibers with PLGA nanoparticles compared to the nanofibers loaded with PHBV [121].

5.5. Role of Growth Factors in Conjunction with Metal-based Composites for rapid bone healing

Yifei et al. plotted a Ti-6Al-4V scaffold, encapsulated with Calcium phosphate (CaP) solution consisting of BMP-2 growth factor and incorporated into muscle pouches of 6 dogs and studied that CaP containing BMP-2 capsules have shown a significant impact on a new bone generation. The outcomes of µ-CT scanning images suggested that the porosity of CaP coated Ti-6Al-4V scaffold decreased from 84.8% to 83.8% in contrast to the Ti-6Al-4V scaffold. Furthermore, the cross-sectional area of the Ti6Al4V scaffold without CaP layering (G1), Ti6Al4V scaffold with CaP coating (G2), and Ti6Al4V scaffold with BMP-2 loaded into the CaP layer (G3) observed that average strut thickness (ST) and coating thickness (CT) is similar for G2 and G3 groups when compared to G1 group and EDX results confirmed the chemical composition of G2 and G3 scaffold as Si, P, Cl, and Ca. After implantation into the dog model, histological analysis revealed that the G3 scaffold resulted in the formation of new bone, surrounded by blood vessels around the network of trabeculae consisting of mineralized bone matrix, osteoblasts, osteoclasts, and osteocytes. In addition, Yifei and the team also reported a uniform bone-to-tissue area (BA/TA) on various samples collected from regions (1m to 5mm) [122]. Hsien-Te Chen developed a Ti-based composite scaffold by coating and immobilizing HAp–TiO2 and BMP-2, respectively, with a pore size between 5 to 0.5 microns. Further, the morphology of prepared scaffolds has depicted a rough surface which favored the increased immobilization of BMP-2. In addition, BMP-2 was released consistently and steadily due to HAp-Ti02 coating

compared to pure Ti with no coating. Furthermore, MC3T3-E1 cells (immature mice osteoblasts) were cultured on prepared scaffolds (pure Ti, Hap-TiO2/Ti BMP-2/Ti, and HAp–TiO2/BMP-2/Ti), and the results of cell attachment (protruded lamellipodia), viability has shown an increased cell response on HAp–TiO2/BMP-2 scaffolds when compared to other three. In addition, enhanced osteogenic properties (increase in ALP expression by qPCR) were also noticed on scaffolds with BMP-2, thus inferring the appropriateness of prepared composite scaffolds for bone tissue engineering applications [123].

6. CONCLUSIONS AND FUTURE STUDIES

From the above work, growth factors are major contributors to tissue engineering applications to achieve the desired level of bone regeneration. Release strategies play a major role in the constant discharge of growth factors instead of burst release, slowing cellular growth as unutilized growth factors are cleaned up from the body through renal filtration. The successful strategies involved using polyelectrolyte systems and porous bio ceramic-polymer composites to deliver growth factors at the defect site effectively. These polymers and bio-ceramic-based growth factory delivery systems were found to be extremely handy and bring the advantage of biodegradability, which eliminates the second surgery involved in the case of metals and non-biodegradable ceramic materials, thereby falling the risk of microbial attack and infection at the site of injury and eases the process for patients as less pain is involved, and regeneration process can be enhanced significantly.

7. ABBREVIATIONS

- BMP - Bone Morphogenetic Protein
- GF - Growth Factor
- TGFβ - Transforming Growth Factor Beta
- VEGF - Vascular Endothelial Growth Factor
- PDGF - Platelet-Derived Growth Factor
- FGF - Fibroblast Growth Factor
- CGF - Concentrated Growth Factor
- TNF - Tumor Necrosis Factor
- CSF - Colony Stimulating Factor
- VWF - Von Willebrand Factor
- PRP - Platelet Rich Plasma
- FDA - Food and Drug Administration
- PEC - Polyelectrolyte Complex
- BTE - Bone Tissue Engineering
- BTR - Bone Tissue Regeneration
- PMMA - Poly Methyl Methacrylate
- PEG - Poly Ethylene Glycol
- PLL - Poly Lysine
- PDA - Poly Dopamine
- PLAGA - Poly Lactide co Glycolide
- PEEK - Poly Ether Ether Ketone
- PEO - Poly Ethylene Oxide
- PHBV - Poly Hydroxy Butyrate - co- Hydroxy Valyrate
- PLA - Poly Lactic Acid
- PCL - Poly Caprolactone
- PGA - Polyglycolic Acid
- PVA - Polyvinyl Alcohol
- PELA - Poly Ethylene Oxide / Lactic Acid
- AEMA - Acetoacetoxy Ethyl Methacrylate
- HAp - Hydroxyapatite
- HCA - Hydroxy Carbonate Apatite
- CHA - Collagen Hydroxyapatite
- β -TCP - Beta Tricalcium Phosphate
- ZrO_2 - Zirconium Dioxide
- Al_2O_3 - Aluminum Oxide
- GC - Glass Ceramic
- CaP - Calcium Phosphate
- BCP - Biphasic Calcium Phosphate
- MSC - Mesenchymal Stem Cell
- HUVEC - Human Umbilical Vein Endothelial Cells
- HGF - Human Gingival Fibroblast
- cEPCs - canine Endothelial Progenitor Cells
- hBFPSCs - human Buccal Fat Pad derived Stem Cells
- HMVEC - Human Dermal Microvascular Endothelial Cells
- hBMSC - Human Bone Marrow Stromal Cells
- hASC - Human Adipose Stem Cells
- SIS - Small Intestine Submucosa
- CS - Chitosan
- SF - Silk Fibroin
- ZA - Zoledronic Acid
- TG - Transglutaminase
- SBF - Simulated Body Fluid
- SEM - Scanning Electron Microscopy
- CLSM - Confocal Laser Scanning Microscopy
- AFM - Atomic Force Microscopy
- BMD - Bone Mineral Density
- CCK - Cell Counting Kit
- GFP - Green Fluorescent Protein
- BSA - Bovine Serum Albumin
- H&E - Hematoxylin and Eosin
- BV - Bone Volume
- TV - Tissue Volume
- OPN - Osteopontin
- OC/OCN - Osteocalcin
- ALP - Alkaline Phosphatase
- IL - Interleukin
- PCR - Polymerase Chain Reaction
- qPCR - quantitative Polymerase Chain Reaction
- RT-PCR - Reverse Transcription based Polymerase Chain Reaction
- CT - Computerized Tomography
- MPa - Megapascals
- GPa – Gigapascals

8. AUTHORS CONTRIBUTION STATEMENT

Yochana, Nikhitha, and Sarvani have prepared the draft, which Kavya edited. Karthik helped with reference works and collecting relevant images. Finally, Nadeem Siddiqui has given the idea, finalized the content, and fine-tuned the entire manuscript.

9. CONFLICT OF INTEREST

Conflict of interest declared none.

10. REFERENCES

1. Biga LM, Dawson S, Harwell A, Hopkins R, Kaufmann J, LeMaster M, et al. 6.3 Bone Structure. In: Anatomy & Physiology. OpenStax/Oregon State University; 2019.
2. Lee DK, Ki MR, Kim EH, Park CJ, Ryu JJ, Jang HS, et al. Biosilicated collagen/β-tricalcium phosphate composites as a BMP-2-delivering bone-graft substitute for accelerated craniofacial bone regeneration. Biomaterials Research. 2021 Apr 21;25(1):1–11.
3. Multi-layered polydopamine coatings for the immobilization of growth factors onto highly-interconnected and bimodal PCL/HA-based scaffolds. Materials Science and Engineering: C. 2020 Dec 1;117:111245.
4. Yifei X, Yanan Y, Li J, Yue M, Hao W, Wang L, et al. Porous composite calcium citrate/polylactic acid materials with high mineralization activity and biodegradability for bone repair tissue engineering. Int J Polym Mater [Internet]. 2021 May 3 [cited 2022 Oct 13]; Available from: https://www.scinapse.io/papers/3010668654
5. NIR fluorescence for monitoring in vivo scaffold degradation along with stem cell tracking in bone tissue engineering. Biomaterials. 2020 Nov 1;258:120267.
6. Glucose cross-linked hydrogels conjugate HA nanorods as bone scaffolds: Green synthesis, characterization and in vitro studies. Mater Chem Phys. 2020 Feb 15;242:122515.
7. Reyes R, la Riva B D, Delgado A, Hernández A, Sánchez E, Évora C. Effect of triple growth factor controlled delivery by a brushite-PLGA system on a bone defect. Injury [Internet]. 2012 Mar [cited 2022 Oct 12];43(3). Available from: https://pubmed.ncbi.nlm.nih.gov/22035848/
8. Nath SD, Abueva C, Kim B, Lee BT. Chitosan-hyaluronic acid polyelectrolyte complex scaffold crosslinked with genipin for immobilization and controlled release of BMP-2. Carbohydr Polym [Internet]. 2015 Jan 22 [cited 2022 Oct 12];115. Available from: https://pubmed.ncbi.nlm.nih.gov/25439881/
9. Narasimhulu CA, Singla DK. The Role of Bone Morphogenetic Protein 7 (BMP-7) in Inflammation in Heart Diseases. Cells [Internet]. 2020 Feb [cited 2022 Oct 13];9(2). Available from: https://www.ncbi.nlm.nih.gov/pmc/articles/PMC7073173/
10. Tong S, Xu DP, Liu ZM, Du Y, Wang XK. Synthesis of the New-Type Vascular Endothelial Growth Factor-Silk Fibroin-Chitosan Three-Dimensional Scaffolds for Bone Tissue Engineering and In Vitro Evaluation. J Craniofac Surg [Internet]. 2016 Mar [cited 2022 Oct 12];27(2). Available from: https://pubmed.ncbi.nlm.nih.gov/26890455/
11. Zhang Y, Cheng N, Miron R, Shi B, Cheng X. Delivery of PDGF-B and BMP-7 by mesoporous bioglass/silk fibrin scaffolds for the repair of osteoporotic defects. Biomaterials [Internet]. 2012 Oct [cited 2022 Oct 12];33(28). Available from: https://pubmed.ncbi.nlm.nih.gov/22763224/
12. De Witte TM, Fratila-Apachitei LE, Zadpoor AA, Peppas NA. Bone tissue engineering via growth factor delivery: from scaffolds to complex matrices. Regen Biomater. 2018 Jun 9;5(4):197–211.
13. Sahoo S, Sinha A, Das M. Synthesis, characterization and in vitro biocompatibility study of strontium titanate ceramic: A potential biomaterial. J Mech Behav Biomed Mater. 2020 Feb;102:103494.
14. Rabiee SM, Nazparvar N, Azizian M, Vashaee D, Tayebi L. Effect of ion substitution on properties of bioactive glasses: A review [Internet]. Vol. 41, Ceramics International. 2015. p. 7241–51. Available from: http://dx.doi.org/10.1016/j.ceramint.2015.02.140
15. Cacciotti I. Bivalent cationic ions doped bioactive glasses: the influence of magnesium, zinc, strontium and copper on the physical and biological properties [Internet]. Vol. 52, Journal of Materials Science. 2017. p. 8812–31. Available from: http://dx.doi.org/10.1007/s10853-017-1010-0
16. Haugen HJ, Lyngstadaas SP, Rossi F, Perale G. Bone grafts: which is the ideal biomaterial? J Clin Periodontol. 2019 Jun;46 Suppl 21:92–102.
17. Mir M, Ali MN, Barakullah A, Gulzar A, Arshad M, Fatima S, et al. Synthetic polymeric biomaterials for wound healing: a review. Progress in Biomaterials. 2018 Feb 14;7(1):1–21.
18. Website [Internet]. Available from: https://royalsocietypublishing.org/doi/10.1098/rsif.2009.0379
19. Chitosan based nanofibers in bone tissue engineering. Int J Biol Macromol. 2017 Nov 1;104:1372–82.
20. Biomimetic approaches in bone tissue engineering: Integrating biological and physicomechanical strategies. Adv Drug Deliv Rev. 2015 Apr 1;84:1–29.
21. Bone morphogenic protein-2 (BMP-2) loaded nanoparticles mixed with human mesenchymal stem cell in fibrin hydrogel for bone tissue engineering. J Biosci Bioeng. 2009 Dec 1;108(6):530–7.
22. Chitosan-based biomaterials for tissue engineering. Eur Polym J. 2013 Apr 1;49(4):780–92.
23. Scaffolds for Bone Tissue Engineering: State of the art and new perspectives. Materials Science and Engineering: C. 2017 Sep 1;78:1246–62.
24. Dang TT, Nikkhah M, Memic A, Khademhosseini A. Polymeric Biomaterials for Implantable Prostheses [Internet]. Natural and Synthetic Biomedical Polymers. 2014. p. 309–31. Available from: http://dx.doi.org/10.1016/b978-0-12-396983-5.00020-x
25. Calcium phosphate ceramic systems in growth factor and drug delivery for bone tissue engineering: A review. Acta Biomater. 2012 Apr 1;8(4):1401–21.
26. Chang PC, Liu BY, Liu CM, Chou HH, Ho MH, Liu HC, et al. Bone tissue engineering with novel rhBMP2-PLLA composite scaffolds. J Biomed Mater Res A. 2007 Jun 15;81(4):771–80.
27. Manring MM, Hawk A, Calhoun JH, Andersen RC. Treatment of War Wounds: A Historical Review [Internet]. Vol. 467, Clinical Orthopaedics & Related Research. 2009. p. 2168–91. Available from: http://dx.doi.org/10.1007/s11999-009-0738-5
28. Hench LL. The story of Bioglass® [Internet]. Vol. 17, Journal of Materials Science: Materials in Medicine. 2006. p. 967–78. Available from: http://dx.doi.org/10.1007/s10856-006-0432-z
29. Website [Internet]. Available from: https://doi.org/10.1111/j.1151-2916.1998.tb02540.x
30. Website [Internet]. Available from: https://doi.org/10.1111/j.1151-2916.1998.tb02540.x
31. Lee K, Silva EA, Mooney DJ. Growth factor delivery-

based tissue engineering: general approaches and a review of recent developments. J R Soc Interface [Internet]. 2011 Feb 6 [cited 2023 Mar 16];8(55). Available from: https://pubmed.ncbi.nlm.nih.gov/20719768/
32. Ferrand A, Eap S, Richert L, Lemoine S, Kalaskar D, Demoustier-Champagne S, et al. Osteogenetic properties of electrospun nanofibrous PCL scaffolds equipped with chitosan-based nanoreservoirs of growth factors. Macromol Biosci. 2014 Jan;14(1):45–55.
33. Sequential delivery of BMP-2 and IGF-1 using a chitosan gel with gelatin microspheres enhances early osteoblastic differentiation. Acta Biomater. 2012 May 1;8(5):1768–77.
34. Peptides for bone tissue engineering. J Control Release. 2016 Dec 28;244:122–35.
35. Varkey M, Gittens SA, Uludag H. Growth factor delivery for bone tissue repair: an update. Expert Opin Drug Deliv [Internet]. 2004 Nov [cited 2023 Mar 16];1(1). Available from: https://pubmed.ncbi.nlm.nih.gov/16296718/
36. Biomimetic hydrogels for controlled biomolecule delivery to augment bone regeneration. Adv Drug Deliv Rev. 2012 Sep 1;64(12):1078–89.
37. Extracellular signaling molecules to promote fracture healing and bone regeneration. Adv Drug Deliv Rev. 2015 Nov 1;94:3–12.
38. Local and targeted drug delivery for bone regeneration. Curr Opin Biotechnol. 2016 Aug 1;40:125–32.
39. Nyberg E, Holmes C, Witham T, Grayson WL. Growth factor-eluting technologies for bone tissue engineering. Drug Deliv Transl Res. 2015 May 13;6(2):184–94.
40. Honda H, Tamai N, Naka N, Yoshikawa H, Myoui A. Bone tissue engineering with bone marrow-derived stromal cells integrated with concentrated growth factor in Rattus norvegicus calvaria defect model. J Artif Organs. 2013 Sep;16(3):305–15.
41. Dyondi D, Webster TJ, Banerjee R. A nanoparticulate injectable hydrogel as a tissue engineering scaffold for multiple growth factor delivery for bone regeneration. Int J Nanomedicine. 2013;8:47–59.
42. de Guzman RC, Saul JM, Ellenburg, Merrill MR, Coan HB, Smith TL, et al. Bone regeneration with BMP-2 delivered from keratose scaffolds. Biomaterials [Internet]. 2013 Feb [cited 2022 Oct 13];34(6). Available from: https://pubmed.ncbi.nlm.nih.gov/23211447/
43. Nandi SK, Kundu B, Basu D. Protein growth factors loaded highly porous chitosan scaffold: a comparison of bone healing properties. Mater Sci Eng C [Internet]. 2013 Apr 1 [cited 2022 Oct 13];33(3). Available from: https://pubmed.ncbi.nlm.nih.gov/23827571/
44. Shi Q, Li Y, Sun J, Zhang H, Chen L, Chen B, et al. The osteogenesis of bacterial cellulose scaffold loaded with bone morphogenetic protein-2. Biomaterials [Internet]. 2012 Oct [cited 2022 Oct 13];33(28). Available from: https://pubmed.ncbi.nlm.nih.gov/22727467/
45. Yu F, Geng D, Kuang Z, Huang S, Cheng Y, Chen Y, et al. Sequentially releasing self-healing hydrogel fabricated with TGFβ3-microspheres and bFGF to facilitate rat alveolar bone defect repair. Asian J Pharm Sci [Internet]. 2022 May [cited 2022 Oct 13];17(3). Available from: https://pubmed.ncbi.nlm.nih.gov/35782329/
46. Controlled delivery of icariin on small intestine submucosa for bone tissue engineering. Materials Science and Engineering: C. 2017 Feb 1;71:260–7.
47. Kim JH, Kim TH, Kang MS, Kim HW. Angiogenic Effects of Collagen/Mesoporous Nanoparticle Composite Scaffold Delivering $VEGF_{165}$. Biomed Res Int [Internet]. 2016 Sep 5 [cited 2022 Oct 13];2016. Available from: https://doi.org/10.1155/2016/9676934
48. Fujioka-Kobayashi M, Schaller B, Kobayashi E, Hernandez M, Zhang Y, Miron RJ. Hyaluronic Acid Gel-Based Scaffolds as Potential Carrier for Growth Factors: An In Vitro Bioassay on Its Osteogenic Potential. J Clin Med Res [Internet]. 2016 Dec [cited 2022 Oct 13];5(12). Available from: https://www.ncbi.nlm.nih.gov/pmc/articles/PMC5184785/
49. Talaei-KhozaniTahereh. Fabrication of platelet-rich plasma/silica scaffolds for bone tissue engineering. Bioinspired, Biomimetic and Nanobiomaterials [Internet]. 2018 Jun 20 [cited 2022 Oct 13]; Available from: https://www.icevirtuallibrary.com/doi/10.1680/jbibn.17.00007
50. Kim BS, Kim JS, Yang SS, Kim HW, Lim HJ, Lee J. Angiogenin-loaded fibrin/bone powder composite scaffold for vascularized bone regeneration. Biomaterials research [Internet]. 2015 Aug 25 [cited 2022 Oct 22];19. Available from: https://pubmed.ncbi.nlm.nih.gov/26331087/
51. Li Q, Zhou G, Yu X, Wang T, Xi Y, Tang Z. Porous deproteinized bovine bone scaffold with three-dimensional localized drug delivery system using chitosan microspheres. Biomed Eng Online [Internet]. 2015 Apr 15 [cited 2022 Oct 22];14. Available from: https://pubmed.ncbi.nlm.nih.gov/25881175/
52. Enzymatic crosslinked gelatin 3D scaffolds for bone tissue engineering. Int J Pharm. 2019 May 1;562:151–61.
53. Azizian S, Hadjizadeh A, Niknejad H. Chitosan-gelatin porous scaffold incorporated with Chitosan nanoparticles for growth factor delivery in tissue engineering. Carbohydr Polym. 2018 Jul 9;202:315–22.
54. Gümüşderelioğlu M, Aday S. Heparin-functionalized chitosan scaffolds for bone tissue engineering. Carbohydr Res [Internet]. 2011 Apr 1 [cited 2022 Oct 22];346(5). Available from: https://pubmed.ncbi.nlm.nih.gov/21333274/
55. Aligned electrospun cellulose scaffolds coated with rhBMP-2 for both in vitro and in vivo bone tissue engineering. Carbohydr Polym. 2019 Jun 1;213:27–38.
56. Park J, Lee SJ, Lee H, Park SA, Lee JY. Three dimensional cell printing with sulfated alginate for improved bone morphogenetic protein-2 delivery and osteogenesis in bone tissue engineering. Carbohydr Polym [Internet]. 2018 Sep 15 [cited 2022 Oct 22];196. Available from: https://pubmed.ncbi.nlm.nih.gov/29891290/
57. Sharmila G, Muthukumaran C, Kirthika S, Keerthana S, Kumar NM, Jeyanthi J. Fabrication and characterization of Spinacia oleracea extract incorporated alginate/carboxymethyl cellulose microporous scaffold for bone tissue engineering. Int J Biol Macromol [Internet]. 2020 Aug 1 [cited 2022 Oct 22];156. Available from: https://pubmed.ncbi.nlm.nih.gov/32294496/
58. Gambari L, Amore E, Raggio R, Bonani W, Barone M, Lisignoli G, et al. Hydrogen sulfide-releasing silk fibroin scaffold for bone tissue engineering. Mater Sci Eng C [Internet]. 2019 Sep [cited 2022 Oct 22];102. Available

from: https://pubmed.ncbi.nlm.nih.gov/31147018/
59. Murphy CM, Schindeler A, Gleeson JP, Yu NY, Cantrill LC, Mikulec K, et al. A collagen-hydroxyapatite scaffold allows for binding and co-delivery of recombinant bone morphogenetic proteins and bisphosphonates. Acta Biomater [Internet]. 2014 May [cited 2022 Oct 22];10(5). Available from: https://pubmed.ncbi.nlm.nih.gov/24456759/
60. Jabbarzadeh E, Deng M, Lv Q, Jiang T, Khan YM, Nair LS, et al. VEGF-incorporated biomimetic poly(lactide-co-glycolide) sintered microsphere scaffolds for bone tissue engineering. J Biomed Mater Res B Appl Biomater [Internet]. 2012 Nov [cited 2022 Oct 13];100(8). Available from: https://pubmed.ncbi.nlm.nih.gov/22915492/
61. Eğri S, Eczacıoğlu N. Sequential VEGF and BMP-2 releasing PLA-PEG-PLA scaffolds for bone tissue engineering: I. Design and in vitro tests. Artif Cells Nanomed Biotechnol [Internet]. 2017 Mar [cited 2022 Oct 13];45(2). Available from: https://pubmed.ncbi.nlm.nih.gov/26912262/
62. Jain S, Meka K Sr, Chatterjee K. Curcumin eluting nanofibers augment osteogenesis toward phytochemical based bone tissue engineering. Biomed Mater [Internet]. 2016 Oct 6 [cited 2022 Oct 13];11(5). Available from: https://pubmed.ncbi.nlm.nih.gov/27710925/
63. Bouyer M, Guillot R, Lavaud J, Plettinx C, Olivier C, Curry V, et al. Surface delivery of tunable doses of BMP-2 from an adaptable polymeric scaffold induces volumetric bone regeneration. Biomaterials [Internet]. 2016 Oct [cited 2022 Oct 13];104. Available from: https://pubmed.ncbi.nlm.nih.gov/27454063/
64. Lee SJ, Lee D, Yoon TR, Kim HK, Jo HH, Park JS, et al. Surface modification of 3D-printed porous scaffolds via mussel-inspired polydopamine and effective immobilization of rhBMP-2 to promote osteogenic differentiation for bone tissue engineering. Acta Biomater [Internet]. 2016 Aug [cited 2022 Oct 13];40. Available from: https://pubmed.ncbi.nlm.nih.gov/26868173/
65. Rampichová M, Buzgo M, Míčková A, Vocetková K, Sovková V, Lukášová V, et al. Platelet-functionalized three-dimensional poly-ε-caprolactone fibrous scaffold prepared using centrifugal spinning for delivery of growth factors. Int J Nanomedicine. 2017;12:347.
66. Rahman M, Peng XL, Zhao XH, Gong HL, Sun XD, Wu Q, et al. 3D bioactive cell-free-scaffolds for in-vitro/in-vivo capture and directed osteoinduction of stem cells for bone tissue regeneration. Bioactive materials [Internet]. 2021 Apr 21 [cited 2022 Oct 22];6(11). Available from: https://pubmed.ncbi.nlm.nih.gov/33997495/
67. Li X, Yi W, Jin A, Duan Y, Min S. Effects of sequentially released BMP-2 and BMP-7 from PELA microcapsule-based scaffolds on the bone regeneration. Am J Transl Res. 2015;7(8):1417.
68. Kim TH, Yun YP, Park YE, Lee SH, Yong W, Kundu J, et al. In vitro and in vivo evaluation of bone formation using solid freeform fabrication-based bone morphogenic protein-2 releasing PCL/PLGA scaffolds. Biomed Mater [Internet]. 2014 Apr [cited 2022 Oct 22];9(2). Available from: https://pubmed.ncbi.nlm.nih.gov/24518200/
69. Murphy WL, Peters MC, Kohn DH, Mooney DJ. Sustained release of vascular endothelial growth factor from mineralized poly(lactide-co-glycolide) scaffolds for tissue engineering. Biomaterials [Internet]. 2000 Dec [cited 2022 Oct 22];21(24). Available from: https://pubmed.ncbi.nlm.nih.gov/11071602/
70. Basmanav FB, Kose GT, Hasirci V. Sequential growth factor delivery from complexed microspheres for bone tissue engineering. Biomaterials [Internet]. 2008 Nov [cited 2022 Oct 22];29(31). Available from: https://pubmed.ncbi.nlm.nih.gov/18691753/
71. Kanczler JM, Ginty PJ, Barry JJ, Clarke NM, Howdle SM, Shakesheff KM, et al. The effect of mesenchymal populations and vascular endothelial growth factor delivered from biodegradable polymer scaffolds on bone formation. Biomaterials [Internet]. 2008 Apr [cited 2022 Oct 22];29(12). Available from: https://pubmed.ncbi.nlm.nih.gov/18234329/
72. Zhang Q, Qin M, Zhou X, Nie W, Wang W, Li L, et al. Porous nanofibrous scaffold incorporated with S1P loaded mesoporous silica nanoparticles and BMP-2 encapsulated PLGA microspheres for enhancing angiogenesis and osteogenesis. J Mater Chem B Mater Biol Med. 2018 Oct 31;6(42):6731–43.
73. Sahoo S, Ang LT, Goh JC, Toh SL. Growth factor delivery through electrospun nanofibers in scaffolds for tissue engineering applications. J Biomed Mater Res A [Internet]. 2010 Jun 15 [cited 2022 Oct 22];93(4). Available from: https://pubmed.ncbi.nlm.nih.gov/20014288/
74. Chen L, Shao L, Wang F, Huang Y, Gao F. Enhancement in sustained release of antimicrobial peptide and BMP-2 from degradable three dimensional-printed PLGA scaffold for bone regeneration. RSC Adv. 2019 Apr 3;9(19):10494–507.
75. RhBMP-2-loaded calcium silicate/calcium phosphate cement scaffold with hierarchically porous structure for enhanced bone tissue regeneration. Biomaterials. 2013 Dec 1;34(37):9381–92.
76. Overman JR, Helder MN, ten Bruggenkate CM, Schulten EA, Klein-Nulend J, Bakker AD. Growth factor gene expression profiles of bone morphogenetic protein-2-treated human adipose stem cells seeded on calcium phosphate scaffolds in vitro. Biochimie [Internet]. 2013 Dec [cited 2022 Oct 13];95(12). Available from: https://pubmed.ncbi.nlm.nih.gov/24028822/
77. Gu Z, Zhang X, Li L, Wang Q, Yu X, Feng T. Acceleration of segmental bone regeneration in a rabbit model by strontium-doped calcium polyphosphate scaffold through stimulating VEGF and bFGF secretion from osteoblasts. Mater Sci Eng C [Internet]. 2013 Jan 1 [cited 2022 Oct 13];33(1). Available from: https://pubmed.ncbi.nlm.nih.gov/25428072/
78. Chen S, Shi Y, Zhang X, Ma J. Evaluation of BMP-2 and VEGF loaded 3D printed hydroxyapatite composite scaffolds with enhanced osteogenic capacity in vitro and in vivo. Mater Sci Eng C [Internet]. 2020 Jul [cited 2022 Oct 13];112. Available from: https://pubmed.ncbi.nlm.nih.gov/32409051/
79. Mijiritsky E, Ferroni L, Gardin C, Bressan E, Zanette G, Piattelli A, et al. Porcine Bone Scaffolds Adsorb Growth Factors Secreted by MSCs and Improve Bone Tissue Repair. Materials [Internet]. 2017 Sep 8 [cited 2022 Oct 13];10(9). Available from: https://pubmed.ncbi.nlm.nih.gov/28885576/
80. Suárez-González D, Lee JS, Diggs A, Lu Y, Nemke B, Markel M, et al. Controlled multiple growth factor

delivery from bone tissue engineering scaffolds via designed affinity. Tissue Eng Part A [Internet]. 2014 Aug [cited 2022 Oct 22];20(15-16). Available from: https://pubmed.ncbi.nlm.nih.gov/24350567/

81. Perez RA, El-Fiqi A, Park JH, Kim TH, Kim JH, Kim HW. Therapeutic bioactive microcarriers: co-delivery of growth factors and stem cells for bone tissue engineering. Acta Biomater [Internet]. 2014 Jan [cited 2022 Oct 22];10(1). Available from: https://pubmed.ncbi.nlm.nih.gov/24121192/
82. Florczyk SJ, Leung M, Jana S, Li Z, Bhattarai N, Huang JI, et al. Enhanced bone tissue formation by alginate gel-assisted cell seeding in porous ceramic scaffolds and sustained release of growth factor. J Biomed Mater Res A [Internet]. 2012 Dec [cited 2022 Oct 13];100(12). Available from: https://pubmed.ncbi.nlm.nih.gov/22767533/
83. Jun SH, Lee EJ, Jang TS, Kim HE, Jang JH, Koh YH. Bone morphogenic protein-2 (BMP-2) loaded hybrid coating on porous hydroxyapatite scaffolds for bone tissue engineering. J Mater Sci Mater Med [Internet]. 2013 Mar [cited 2022 Oct 13];24(3). Available from: https://pubmed.ncbi.nlm.nih.gov/23344924/
84. Su Y, Su Q, Liu W, Lim M, Venugopal JR, Mo X, et al. Controlled release of bone morphogenetic protein 2 and dexamethasone loaded in core-shell PLLACL-collagen fibers for use in bone tissue engineering. Acta Biomater [Internet]. 2012 Feb [cited 2022 Oct 13];8(2). Available from: https://pubmed.ncbi.nlm.nih.gov/22100346/
85. Fujioka-Kobayashi M, Ota MS, Shimoda A, Nakahama K, Akiyoshi K, Miyamoto Y, et al. Cholesteryl group- and acryloyl group-bearing pullulan nanogel to deliver BMP2 and FGF18 for bone tissue engineering. Biomaterials [Internet]. 2012 Oct [cited 2022 Oct 13];33(30). Available from: https://pubmed.ncbi.nlm.nih.gov/22800537/
86. Comparative study of osteogenic potential of a composite scaffold incorporating either endogenous bone morphogenetic protein-2 or exogenous phytomolecule icaritin: An in vitro efficacy study. Acta Biomater. 2012 Aug 1;8(8):3128–37.
87. Farokhi M, Mottaghitalab F, Ai J, Shokrgozar MA. Sustained release of platelet-derived growth factor and vascular endothelial growth factor from silk/calcium phosphate/PLGA based nanocomposite scaffold. Int J Pharm [Internet]. 2013 Sep 15 [cited 2022 Oct 13];454(1). Available from: https://pubmed.ncbi.nlm.nih.gov/23856159/
88. Santo VE, Duarte AR, Popa EG, Gomes ME, Mano JF, Reis RL. Enhancement of osteogenic differentiation of human adipose derived stem cells by the controlled release of platelet lysates from hybrid scaffolds produced by supercritical fluid foaming. J Control Release [Internet]. 2012 Aug 20 [cited 2022 Oct 13];162(1). Available from: https://pubmed.ncbi.nlm.nih.gov/22698936/
89. Lu H, Kawazoe N, Kitajima T, Myoken Y, Tomita M, Umezawa A, et al. Spatial immobilization of bone morphogenetic protein-4 in a collagen-PLGA hybrid scaffold for enhanced osteoinductivity. Biomaterials [Internet]. 2012 Sep [cited 2022 Oct 13];33(26). Available from: https://pubmed.ncbi.nlm.nih.gov/22698726/
90. Choi DH, Park CH, Kim IH, Chun HJ, Park K, Han DK. Fabrication of core-shell microcapsules using PLGA and alginate for dual growth factor delivery system. J Control Release [Internet]. 2010 Oct 15 [cited 2022 Oct 13];147(2). Available from: https://pubmed.ncbi.nlm.nih.gov/20647022/
91. Biomimetic gelatin/chitosan/polyvinyl alcohol/nano-hydroxyapatite scaffolds for bone tissue engineering. Mater Des. 2021 Sep 1;207:109865.
92. Development of PLGA-coated β-TCP scaffolds containing VEGF for bone tissue engineering. Materials Science and Engineering: C. 2016 Dec 1;69:780–8.
93. Bastami F, Paknejad Z, Jafari M, Salehi M, Rezai RM, Khojasteh A. Fabrication of a three-dimensional β-tricalcium-phosphate/gelatin containing chitosan-based nanoparticles for sustained release of bone morphogenetic protein-2: Implication for bone tissue engineering. Mater Sci Eng C [Internet]. 2017 Mar 1 [cited 2022 Oct 13];72. Available from: https://pubmed.ncbi.nlm.nih.gov/28024612/
94. Sobhani A, Rafienia M, Ahmadian M, Naimi-Jamal M. Fabrication and Characterization of Polyphosphazene/Calcium Phosphate Scaffolds Containing Chitosan Microspheres for Sustained Release of Bone Morphogenetic Protein 2 in Bone Tissue Engineering. 2017 [cited 2022 Oct 13]; Available from: https://doi.org/10.1007/s13770-017-0056-z
95. Lei Y, Xu Z, Ke Q, Yin W, Chen Y, Zhang C, et al. Strontium hydroxyapatite/chitosan nanohybrid scaffolds with enhanced osteoinductivity for bone tissue engineering. Mater Sci Eng C [Internet]. 2017 Mar 1 [cited 2022 Oct 13];72. Available from: https://pubmed.ncbi.nlm.nih.gov/28024569/
96. Lin H, Tang Y, Lozito TP, Oyster N, Kang RB, Fritch MR, et al. Projection Stereolithographic Fabrication of BMP-2 Gene-activated Matrix for Bone Tissue Engineering. Sci Rep. 2017 Sep 12;7(1):1–11.
97. Gentile P, Nandagiri VK, Daly J, Chiono V, Mattu C, Tonda-Turo C, et al. Localised controlled release of simvastatin from porous chitosan-gelatin scaffolds engrafted with simvastatin loaded PLGA-microparticles for bone tissue engineering application. Mater Sci Eng C [Internet]. 2016 Feb [cited 2022 Oct 13];59. Available from: https://pubmed.ncbi.nlm.nih.gov/26652371/
98. Chiu YC, Fong EL, Grindel BJ, Kasper FK, Harrington DA, Farach-Carson MC. Sustained delivery of recombinant human bone morphogenetic protein-2 from perlecan domain I - functionalized electrospun poly (ε-caprolactone) scaffolds for bone regeneration. Journal of experimental orthopaedics [Internet]. 2016 Dec [cited 2022 Oct 13];3(1). Available from: https://pubmed.ncbi.nlm.nih.gov/27714703/
99. Patntirapong S, Janvikul W, Theerathanagorn T, Singhatanadgit W. Osteoinduction of stem cells by collagen peptide-immobilized hydrolyzed poly(butylene succinate)/β-tricalcium phosphate scaffold for bone tissue engineering. J Biomater Appl [Internet]. 2017 Jan [cited 2022 Oct 13];31(6). Available from: https://pubmed.ncbi.nlm.nih.gov/30208806/
100. Zhao X, Han Y, Li J, Cai B, Gao H, Feng W, et al. BMP-2 immobilized PLGA/hydroxyapatite fibrous scaffold via polydopamine stimulates osteoblast growth. Mater Sci Eng C [Internet]. 2017 Sep 1 [cited 2022 Oct 13];78. Available from: https://pubmed.ncbi.nlm.nih.gov/28576035/
101. Cao L, Yu Y, Wang J, Werkmeister JA, McLean KM, Liu C. 2-N, 6-O-sulfated chitosan-assisted BMP-2

immobilization of PCL scaffolds for enhanced osteoinduction. Mater Sci Eng C [Internet]. 2017 May 1 [cited 2022 Oct 13];74. Available from: https://pubmed.ncbi.nlm.nih.gov/28254298/

102. Zhang HX, Zhang XP, Xiao GY, Hou Y, Cheng L, Si M, et al. In vitro and in vivo evaluation of calcium phosphate composite scaffolds containing BMP-VEGF loaded PLGA microspheres for the treatment of avascular necrosis of the femoral head. Mater Sci Eng C [Internet]. 2016 Mar [cited 2022 Oct 13];60. Available from: https://pubmed.ncbi.nlm.nih.gov/26706534/
103. Bae MS, Ko NR, Lee SJ, Lee JB, Heo DN, Byun W, et al. Development of novel photopolymerizable hyaluronic acid/heparin-based hydrogel scaffolds with a controlled release of growth factors for enhanced bone regeneration. Macromol Res. 2016 Aug 11;24(9):829–37.
104. Quinlan E, López-Noriega A, Thompson E, Kelly HM, Cryan SA, O'Brien FJ. Development of collagen-hydroxyapatite scaffolds incorporating PLGA and alginate microparticles for the controlled delivery of rhBMP-2 for bone tissue engineering. J Control Release [Internet]. 2015 Jan 28 [cited 2022 Oct 22];198. Available from: https://pubmed.ncbi.nlm.nih.gov/25481441/
105. Zheng L, Wang L, Qin J, Sun X, Yang T, Ni Y, et al. New Biodegradable Implant Material Containing Hydrogel with Growth Factors of Lyophilized PRF in Combination with an nHA/PLGA Scaffold. J Hard Tissue Biol. 2015;24(1):54–60.
106. Wang Z, Wang K, Lu X, Li M, Liu H, Xie C, et al. BMP-2 encapsulated polysaccharide nanoparticle modified biphasic calcium phosphate scaffolds for bone tissue regeneration. J Biomed Mater Res A [Internet]. 2015 Apr [cited 2022 Oct 22];103(4). Available from: https://pubmed.ncbi.nlm.nih.gov/25100662/
107. He X, Liu Y, Yuan X, Lu L. Enhanced healing of rat calvarial defects with MSCs loaded on BMP-2 releasing chitosan/alginate/hydroxyapatite scaffolds. PLoS One [Internet]. 2014 Aug 1 [cited 2022 Oct 22];9(8). Available from: https://pubmed.ncbi.nlm.nih.gov/25084008/
108. Fan J, Park H, Lee MK, Bezouglaia O, Fartash A, Kim J, et al. Adipose-derived stem cells and BMP-2 delivery in chitosan-based 3D constructs to enhance bone regeneration in a rat mandibular defect model. Tissue Eng Part A [Internet]. 2014 Aug [cited 2022 Oct 22];20(15-16). Available from: https://pubmed.ncbi.nlm.nih.gov/24524819/
109. Sheehy EJ, Miller GJ, Amado I, Raftery RM, Chen G, Cortright K, et al. Mechanobiology-informed regenerative medicine: Dose-controlled release of placental growth factor from a functionalized collagen-based scaffold promotes angiogenesis and accelerates bone defect healing. J Control Release [Internet]. 2021 Jun 10 [cited 2022 Oct 22];334. Available from: https://pubmed.ncbi.nlm.nih.gov/33811984/
110. Wang G, Qiu J, Zheng L, Ren N, Li J, Liu H, et al. Sustained delivery of BMP-2 enhanced osteoblastic differentiation of BMSCs based on surface hydroxyapatite nanostructure in chitosan-HAp scaffold. J Biomater Sci Polym Ed [Internet]. 2014 [cited 2022 Oct 22];25(16). Available from: https://pubmed.ncbi.nlm.nih.gov/25166866/
111. In Situ Controlled Release of rhBMP-2 in Gelatin-Coated 3D Porous Poly(ε-caprolactone) Scaffolds for Homogeneous Bone Tissue Formation - Google Search [Internet]. [cited 2022 Oct 22]. Available from: https://www.google.com/search?q=In+Situ+Controlled+Release+of+rhBMP-2+in+Gelatin-Coated+3D+Porous+Poly(%CE%B5-caprolactone)+Scaffolds+for+Homogeneous+Bone+Tissue+Formation&rlz=1C1CHBF_enIN1020IN1020&oq=In+Situ+Controlled+Release+of+rhBMP-2+in+Gelatin-Coated+3D+Porous+Poly(%CE%B5-caprolactone)+Scaffolds+for+Homogeneous+Bone+Tissue+Formation&aqs=chrome..69i57j69i64l2.1288j0j4&sourceid=chrome&ie=UTF-8
112. Osseointegration evaluation of UHMWPE and PEEK-based scaffolds with BMP-2 using model of critical-size cranial defect in mice and push-out test. J Mech Behav Biomed Mater. 2021 Jul 1;119:104477.
113. Controlled growth factor delivery system with osteogenic-angiogenic coupling effect for bone regeneration. Journal of Orthopaedic Translation. 2021 Nov 1;31:110–25.
114. Bal Z, Korkusuz F, Ishiguro H, Okada R, Kushioka J, Chijimatsu R, et al. A novel nano-hydroxyapatite/synthetic polymer/bone morphogenetic protein-2 composite for efficient bone regeneration. Spine J [Internet]. 2021 May [cited 2022 Oct 22];21(5). Available from: https://pubmed.ncbi.nlm.nih.gov/33493682/
115. Kong X, Wang J, Cao L, Yu Y, Liu C. Enhanced osteogenesis of bone morphology protein-2 in 2-N,6-O-sulfated chitosan immobilized PLGA scaffolds. Colloids Surf B Biointerfaces [Internet]. 2014 Oct 1 [cited 2022 Oct 22];122. Available from: https://pubmed.ncbi.nlm.nih.gov/25084565/
116. Mussel-inspired hybrid coating functionalized porous hydroxyapatite scaffolds for bone tissue regeneration. Colloids Surf B Biointerfaces. 2019 Jul 1;179:470–8.
117. Thomas A, Johnson E, Agrawal AK, Bera J. Preparation and characterization of glass–ceramic reinforced alginate scaffolds for bone tissue engineering. J Mater Res. 2019 Nov;34(22):3798–809.
118. Hu Y, Zheng L, Zhang J, Lin L, Shen Y, Zhang X, et al. Dual delivery of bone morphogenetic protein-2 and basic fibroblast growth factor from nanohydroxyapatite/collagen for bone tissue engineering. Applied Biological Chemistry. 2019 Sep 27;62(1):1–9.
119. 3D printing of silk fibroin-based hybrid scaffold treated with platelet rich plasma for bone tissue engineering. Bioactive Materials. 2019 Dec 1;4:256–60.
120. Surface functionalization of dual growth factor on hydroxyapatite-coated nanofibers for bone tissue engineering. Appl Surf Sci. 2020 Aug 1;520:146311.
121. Yilgor P, Tuzlakoglu K, Reis RL, Hasirci N, Hasirci V. Incorporation of a sequential BMP-2/BMP-7 delivery system into chitosan-based scaffolds for bone tissue engineering. Biomaterials [Internet]. 2009 Jul [cited 2022 Oct 22];30(21). Available from: https://pubmed.ncbi.nlm.nih.gov/19361857/
122. BMP-2 incorporated biomimetic CaP coating functionalized 3D printed Ti6Al4V scaffold induces ectopic bone formation in a dog model. Mater Des. 2022 Mar 1;215:110443.
123. Assessment of bone morphogenic protein and hydroxyapatite–titanium dioxide composites for bone implant materials. Surf Coat Technol. 2015 Aug 25;276:168–74.